Modeling the effects of two different land cover change data sets on the carbon stocks of plants and soils in concert with CO_2 and climate change

Atul K. Jain and Xiaojuan Yang

Department of Atmospheric Science, University of Illinois, Urbana, Illinois, USA

[1] A geographically explicit terrestrial carbon cycle component of the Integrated Science Assessment Model (ISAM) is used to examine the response of plant and soil carbon stocks to historical changes in cropland land cover, atmospheric CO_2, and climate. The ISAM model is forced with two different land cover change data sets for cropland: one spatially resolved set based on cropland statistics (Ramankutty and Foley, 1998, 1999) and another regionally specific set based on deforestation rates (Houghton and Hackler, 1999, 2001; Houghton, 1999, 2000, 2003). To our knowledge, this is the first attempt to incorporate Houghton's regionally specific land cover change data into a spatially resolved terrestrial model. Our model results indicate that globally aggregated land use emissions are not sensitive to the spatially explicit location of the natural vegetation converted for croplands within a region. The ISAM estimated land use emissions based on Houghton's data were substantially higher during the 1980s than those based on Ramankutty and Foley's data. Although our results are consistent with previous model results, they do not support the ideas that the differences between the two land use emissions for cropland changes can either be related to modeling framework or global land use practices. This study suggests that differences between the two sets of land use fluxes are primarily due to the differences in the rates of changes in land area amount for croplands. The ISAM model estimates a larger contribution to net CO_2 uptake from CO_2 fertilization (-2.0 GtC/yr), and a smaller contribution from biospheric CO_2 release due to the climate effect (0.7 GtC/yr) during the 1980s. The negative CO_2 fertilization feedback is most pronounced in the tropics and midlatitudes, whereas the positive temperature effect on CO_2 uptake is most pronounced in the high-latitude regions of the Northern Hemisphere. The ISAM estimated land use emissions due to land cover changes for croplands and pasturelands during the 1980s vary between 1.60 and 2.06 GtC/yr. Most importantly, Intergovernmental Panel on Climate Change estimates based on the CO_2 and O_2 data indicate that terrestrial ecosystems become a sink for atmospheric CO_2 in the 1980s (-0.2 ± 0.7 GtC/yr), whereas they remain a source in simulations based on the ISAM (0.63 ± 0.20 GtC/yr). Our results leave open the possibility that the discrepancy in the magnitudes of the modeled and data-based net terrestrial uptakes for the 1980s decade reflect weaknesses in the terrestrial biosphere model and/or uncertainties in the land cover, O_2 data, or data-based estimates.

1. Introduction

[2] Human activities have significantly altered the Earth's vegetation cover in nearly every part of the world. Such changes have considerable consequences for the health and resilience of land ecosystems [*Marland et al.*, 2003]. They also have the potential to alter regional and global climate through changes in the biophysical characteristics of the Earth's surface, such as albedo and surface roughness [*Ramankutty and Foley*, 1999], and changes in the global carbon cycle. The terrestrial ecosystems have in the past been and may become a source of atmospheric CO_2 generating significant perturbation of the global carbon cycle through emission of CO_2. Recognizing the importance of land ecosystems in the global carbon cycle and the impact of increasing atmospheric carbon dioxide concentrations on global climate, the *United Nations Framework*

Convention on Climate Change (*UNFCC*) [1997] calls for the protection, enhancement, and quantification of terrestrial biospheric sinks for anthropogenic CO_2 emissions [*Cramer et al.*, 2001].

[3] Modeling and measurement studies indicate that ocean and land ecosystems are currently absorbing slightly more than 50% of the human fossil CO_2 emissions [*Prentice et al.*, 2001]. However, a significant question remains regarding those sources and sinks determined primarily by changes in land use. Analyses of terrestrial carbon storage based on these changes have consistently shown a net loss of carbon globally. However, according to some studies [*Schimel et al.*, 2001; *Pacala*, 2001; *Houghton*, 2003] some regions, particularly North America and Eurasia, have actually accumulated carbon. In spite of the importance of land use changes in determining the long-term carbon sources and sinks over land, estimates of the land use carbon flux term have the largest uncertainties in the global carbon budget equation [*Prentice et al.*, 2001]. This is mainly due to poor characterization of the extent and nature of global land use practices, and uncertainty in the amount of carbon released to the atmosphere following such practices.

[4] As a result, recent estimates of the land use emissions have been published with relatively large differences in the results. In the most recent Intergovernmental Panel on Climate Change report [*Prentice et al.*, 2001], the estimates of land use emissions based on the model calculations using cropland statistics from the United Nations Food and Agriculture Organization (FAO) [*Ramankutty and Foley*, 1998, 1999] (hereinafter referred to as RF) and deforestation rates from the FAO Forest Resource Assessment FRA [*Houghton and Hackler*, 1999, 2001; *Houghton*, 1999, 2000] (hereinafter referred to as HH) over the last 50 years differ widely [*Prentice et al.*, 2001]. Results based on four processes-based models using RF data for cropland statistics show maximum increase around 1960 with a progressively decreasing release till 1992, the final year of data availability (The Carbon Cycle Model Linkage Project, CCMLP, study [*McGuire et al.*, 2001]). In contrast, land use emissions based on a bookkeeping model using HH data for deforestation rates show a generally increasing rate of emissions reaching a maximum between 1950 and the present [*Houghton*, 2003].

[5] The authors of these two data sets proposed various hypotheses for the difference between these two data sets. *House et al.* [2003] suggest that the differences in the land use emissions may be due to the fact that these estimates were carried out using different types of models and diverse sets of land cover change activities and data sets. HH's land use emissions estimates using the FAO deforestation rates were based on a bookkeeping model that balances deforestation and forest regrowth over time, assuming no temporal variations in environmental factors, such as CO_2, nitrogen deposition, or climate [*Houghton*, 2003]. On the other hand, CCMLP estimates used cropland density data together with four process-based models, which took into account the concurrent effects of increase in atmospheric CO_2 and climate change [*McGuire et al.*, 2001]. *House et al.* [2003] and *McGuire et al.* [2001] also suggest that HH

data-based estimates higher because HH data analysis included conversion of forests to pastures in addition to cropland establishment/abandonment [*Houghton*, 1999, 2000], whereas the CCMLP study [*McGuire et al.*, 2001] considered cropland establishment/abandonment only. While the causes of difference in land use emissions have been proposed, they have not yet been evaluated using the terrestrial ecosystem models. Accordingly, one of the purposes of this study is to evaluate uncertainties in the land use emissions and net land-atmosphere fluxes by forcing a single terrestrial model with two different land cover change data sets for cropland changes. This approach allows us to isolate the cropland change data related uncertainties from the model related uncertainties in the terrestrial biospheric fluxes. The evaluation of two alternative data sets for historical changes in land cover is important because the flux associated with land cover change is responsible for substantial uncertainty in net land-atmosphere flux for the recent decades.

[6] In particular, there are three main objectives of this study: (1) to estimate the land use emissions for CO_2 and net land-atmosphere CO_2 fluxes using two different land cover data sets for croplands (HH and RF data sets), each being used to drive the terrestrial carbon cycle component of the Integrated Science Assessment Model (ISAM) [*Jain et al.*, 1996; *Kheshgi and Jain*, 2003] coupled with observed atmospheric CO_2, temperature, and precipitation data; (2) to examine a number of hypotheses proposed by the authors of these two data sets for the differences between them [*McGuire et al.*, 2001; *House et al.*, 2003]; and (3) to discuss sources of uncertainties in these two data sets and model results, and the potential for reduction of these uncertainties.

[7] The paper is organized as follows: Section 2 provides a brief description of the methodology used to calculate plant and soil carbon stocks using the ISAM terrestrial model, along with a discussion of the climate, atmospheric CO_2, land cover changes, and natural vegetation distribution data used in this study. In section 3 we report the global and annual mean ISAM based results for terrestrial biosphere fluxes associated with changes in land use, climate, and atmospheric CO_2 over the period 1900–1990 and for the 1980s. Section 4 compares ISAM model results with other model studies. Finally, the major findings of this study are provided in section 5, accompanied by a discussion and summary of key results.

2. Methods

2.1. Terrestrial Biosphere Model Description

[8] Given our lack of understanding of the mechanisms that drive terrestrial ecosystems, the extent to which a carbon cycle model can reliably project the historical and future behavior of the real world remains limited. The purpose of the model we use in this study is to represent the current state-of-the-art knowledge of terrestrial ecosystems while at the same time studying the effects of human-induced land use emissions on terrestrial ecosystems and related resources, in addition to addressing how interactions with climate and changes occurring due to climate change

Table 1. Net Primary Productivity and Vegetation, Soil, and Total Carbon Storage by Land Cover Type in 1765

Land Cover Type	Net Primary Product (NPP)		Vegetation Carbon (VC)		Soil Organic Carbon (SOC)		Total Carbon (TC)	
	kgC m^{-2}yr^{-1}	GtC/yr	kgC m^{-2}	GtC	kgC m^{-2}	GtC	kgC m^{-2}	GtC
Tropical evergreen	1.07	13.7	20.87	268	10.65	133	31.53	401
Tropical deciduous	0.77	6.0	16.54	128	5.96	50	22.50	178
Temperate evergreen	1.02	5.1	21.50	109	14.03	73	35.53	182
Temperate deciduous	0.98	5.0	21.27	108	11.00	35	32.27	143
Boreal	0.32	6.4	7.07	142	26.26	496	33.34	638
Savanna	0.81	9.7	2.01	24	19.22	206	21.23	230
Grassland	0.15	4.0	0.33	9	4.67	131	5.00	140
Shrubland	0.22	3.2	0.82	12	8.78	110	9.61	122
Tundra	0.13	1.2	0.73	7	21.74	241	22.47	248
Desert	0.09	0.7	0.60	5	5.60	34	6.20	39
Polar ice/desert	0.00	0.0	0.00	0	11.64	5	11.64	54
Cropland	0.38	3.3	1.62	14	1.60	39	3.21	53
Pastureland	0.12	1.0	1.46	13	2.86	40	4.32	53
Total		59.3		838		1594		2432

could affect the terrestrial ecosystems. This model is an extended version of our coupled climate–carbon cycle component of the one-dimensional version of the Integrated Science Assessment Model (ISAM-1D), which was used to reconstruct the past carbon cycle and isotopic variations in the atmosphere, terrestrial biosphere, and oceans, in addition to estimating the uncertainty in the global carbon budget, and which has been described elsewhere [*Jain et al.*, 1995, 1996, 1997; *Jain and Hayhoe*, 2003; *Kheshgi et al.*, 1999; *Kheshgi and Jain*, 2003; *Prentice et al.*, 2001]. The earlier version of the ISAM carbon cycle model has also been used in recent and past assessments of the Intergovernmental Panel on Climate Change [*Schimel et al.*, 1996; *Prentice et al.*, 2001].

2.1.1. General Structure of the Terrestrial Carbon Cycle Model

[9] The extended version of the ISAM model simulates the carbon fluxes to and from different compartments of the terrestrial biosphere with 0.5-by-0.5 degree spatial resolution. Each grid cell is completely occupied by at least one of the twelve natural land coverage classifications and/or croplands. The natural vegetation types considered in this study represent both highly managed and less managed land cover types (Table 1). Each grid is also assigned one of the 105 soil types based on the FAO-UNESCO Soil Map of the World [*Zobler*, 1986, 1999]. Within each grid cell, the carbon dynamics of each land-coverage classification is described by a model of carbon in vegetation and soil, which is depicted in Figure 1. The model consists of three vegetation carbon reservoirs (ground vegetation (GV), nonwoody tree part (NWT), and woody tree parts (WT)), two litter reservoirs (decomposable plant material (DPM) and resistant material (RPM)), and three soil reservoirs (microbial biomass BIO), humified organic matter (HUM), and inert organic matter (IOM)). This model structure, which is based on major elements of terrestrial ecosystems, allows consistent analysis of carbon fluxes due to forest clearing and land cover changes.

2.1.2. Vegetation Carbon and NPP

[10] The vegetation carbon density (kgC m^{-2}) of each land cover type including croplands within each grid cell is the difference between net primary productivity (NPP) and

losses through litterfall, and herbivore consumption. In the model, NPP (kg C m^{-2} yr^{-1}, the photosynthetically fixed carbon minus the autotrophic respiration) by ground vegetation and trees varies with vegetation carbon according to plant growth equations [*Jain et al.*, 1996; *Kheshgi et al.*, 1996; *King et al.*, 1995]. The GV and NWT reservoirs fix carbon by photosynthesis while all three vegetation reservoirs release carbon by respiration. The three vegetation carbon reservoirs are characterized by their turnover times and the rate of exchange between them. The values of these
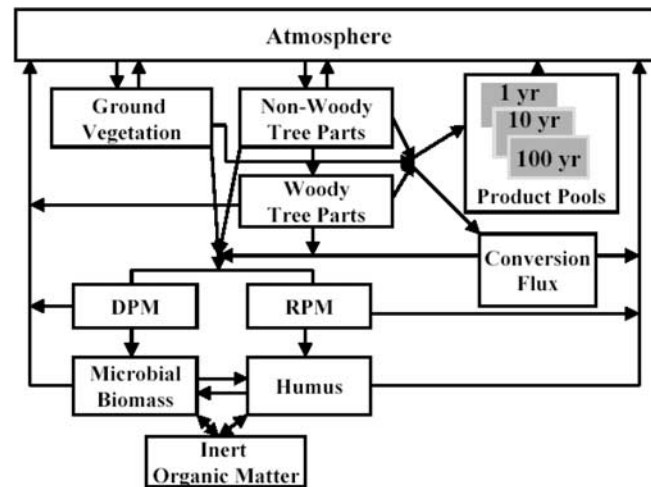

Figure 1. Schematic diagram of the terrestrial ecosystem component of the Integrated Science Assessment Model (ISAM). Ground vegetation, nonwoody, and woody tree parts represent vegetation carbon pools. DPM and RPM are easily decomposable resistant aboveground and belowground litter pools. The three soil pools are microbial, humus, and inert organic matters. The conversion carbon fluxes are associated with the land cover changes representing slash carbon left on the ground that is consecutively transferred to litter pools, and carbon released from burning of plant material. The part of the biomass harvested is transferred to three product pools with different turnover times.

parameters for each of our model's land cover types are calculated from the specified initial values of fraction of tree [*Zhu and Waller*, 2003] and ground vegetation carbon (kgC m^{-2} yr^{-1}) [*Schlesinger*, 1997; *Bolin et al.*, 2000]. The vegetation carbon partitioned into three vegetation reservoirs (GV, NWT, and WT) is based on the global ratios of the contents of these reservoirs [*Jain et al.*, 1996]. Table 1 provides the initial carbon contents for various land cover types.

[11] The increase in the rate of photosynthesis by terrestrial biota, relative to preindustrial times (1765), is thought to be stimulated by increasing atmospheric CO_2 concentrations. In the previous version of the ISAM [*Jain et al.*, 1996, *Kheshgi and Jain*, 2003], this increase was modeled using the frequently used logarithmic function of *Bacastow and Keeling* [1973],

$$\text{NPP}(t) = \text{NPP}_0\left(1 + \beta_1 \ln\left(\frac{CO_2(t)}{CO_2(0)}\right)\right), \qquad (1)$$

where $CO_2(0)$ and $CO_2(t)$ are the CO_2 concentrations at the pre-industrial time and at time t. β_1 is the biotic growth factor, which may vary with vegetation type but does not itself change with atmospheric CO_2. NPP_0 and $\text{NPP}(t)$ are the NPP at the pre-industrial time and at time t.

[12] The logarithmic function of equation (1) has been criticized for its poor representation of C_3 plants' physiological response to elevated CO_2 [*Gates*, 1985], whereas the biotic growth factor could also vary with changes in CO_2 concentrations and temperatures. Therefore we replaced the logarithmic function by the function of *King et al.* [1995] and constant biotic growth factor by *Polglase and Wang*'s [1992] derived growth factor (β_2) based on the biochemical model of *Farquhar and von Caemmerer* [1982],

$$\text{NPP}(t) = \text{NPP}_0\left(1 + \beta_2 \frac{CO_2(t) - CO_2(0)}{CO_2(0)}\right)$$

$$\beta_2 = \frac{3\chi CO_2(t)\Gamma^*}{(\chi CO_2(t) - \Gamma^*)(\chi CO_2(t) + 2\Gamma^*)},$$

where $\chi = CO_2(t)_i/CO_2(t)$, and $CO_2(t)_i$ is the intercellular CO_2 concentration. On the basis of the measurements of *King et al.* [1995], the estimated values of $\chi = 0.7$ for C_3 plants and 0.4 for C4 plants were used in this study. We assumed that grasslands were 100% C_4 plants and savannas were 75% C_4 plants. β_2 was estimated for these two biomes by first calculating their respective β_2 as if they were pure C_3 biomes, then reducing these estimates by 50% [*Polglase and Wang*, 1992]. Γ^* is the CO_2 compensation point in the absence of day respiration, which is assumed as a function of temperature for C_3 plants [*Post et al.*, 1997].

[13] Note that β_2 is a decreasing function of atmospheric CO_2 and increasing function of temperature [*Polglase and Wang*, 1992]. While NPP may increase with increasing CO_2, the rate of increase per increase in atmospheric CO_2 will decline if the temperature is constant but can increase with increasing temperature.

[14] The vegetation component of the model contains temperature feedback through the respiration and photosynthesis rates to and from the vegetation reservoirs, which follow the Q_{10} formulation described by *Kheshgi et al.* [1996]. In the model, increases in either temperature or CO_2 lead to increases in NPP for ground vegetation and nonwoody tree parts reservoirs.

2.1.3. Litter and Soil Carbon

[15] The litter and soil carbon dynamics are estimated based on the Rothamsted soil turnover model [*Jenkinson*, 1990]. The model essentially consists of five reservoirs (two litter reservoirs, DPM and RPM, and three soil reservoirs, BIO, HUM, IOM) with separate organic carbon reservoirs (Figure 1). This model uses monthly plant material as an input. The incoming plant material enters the litter reservoirs (DPM is easily decomposable plant material, and RPM is resistant plant material) and undergoes decomposition and releases CO_2. The decomposed material is then distributed into the atmosphere, BIO, and HUM reservoirs. When the substrate is attacked it is assumed that the ratio of BIO to HUM formed is the same for all soils. When BIO and HUM decompose, CO_2, BIO, and HUM are formed again in the same proportions. The soil is also assumed to contain a small amount of inert organic matter (IOM) in a separate reservoir. The exchange rates of carbon are modified by environmental factors including temperature, soil moisture deficit, soil temperature, and the plant protection factors. The decomposition rates are temperature dependent according to *Post et al.* [1997]. In the soil model, the plant protection factor is assumed to be 0.6 in all our simulations. The soil moisture deficit function, the difference between soil moisture at field capacity and actual soil moisture, is assumed to vary from 0.0 to 1.0. It is 1.0 for pressure ranging from field capacity (millimeters water held at -33 kPa tension) to a soil water pressure of -100 kPa. In this study, the soil moisture function decreases linearly from 1.0 at -100 kPa to 0.2 at a soil moisture deficit with a tension of -1500 kPa.

2.1.4. Soil Moisture Deficit

[16] Soil moisture deficit is the difference between soil moisture at field capacity (i.e., potential soil moisture) and actual soil moisture. We calculate actual soil water (mm) and soil water pressure (kPa) for each grid cell with the monthly climatic water budget model of *Thornthwaite and Mather* [1957] as implemented by *Pastor and Post* [1985]. The soil hydraulic characteristics for the Rothamsted soil moisture function and the *Thornthwaite and Mather* [1957] water balance calculations are derived from soil depth and texture information for each FAO soil type [*Zobler*, 1986, 1999], rooting depth estimates [*Webb et al.*, 1991], and relationships between soil texture and water content at the critical pressure [*Rawls et al.*, 1982].

2.1.5. Land Use Emissions

[17] In this study we consider two types of land cover change activities: clearing of natural ecosystems for croplands, and recovery of abundant croplands to pre-conversion natural vegetation. The land use emissions due to land cover change activities are calculated using the same bookkeeping approach as *Houghton et al.* [1983] for modeling ecosystems affected by land-use changes. In their model, annual changes
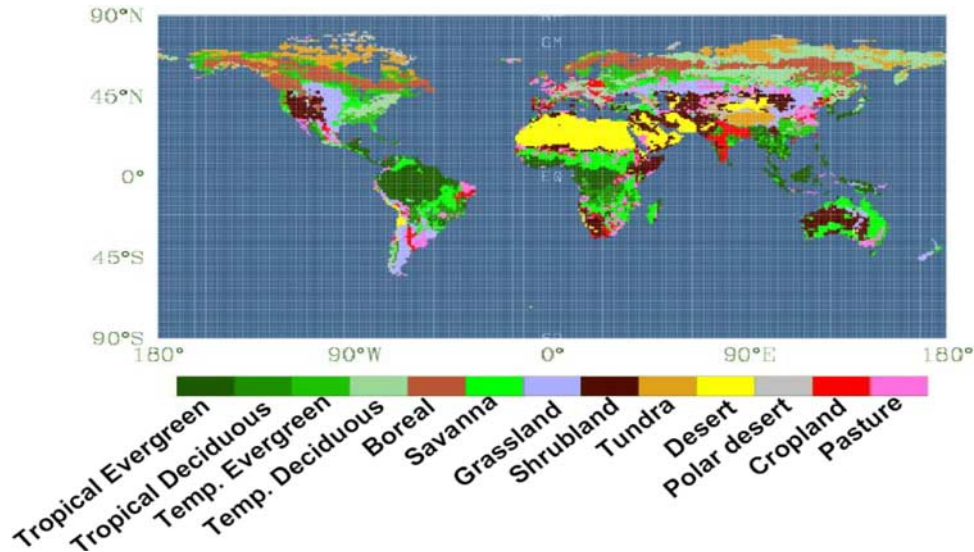
Figure 2. Spatial distribution of the natural vegetation types for the year 1765 that was used to drive the ISAM in this study.

in vegetation and soil following the land cover changes were prescribed using the synoptic response curves for different ecosystems. However, in this study the changes in carbon stocks following the land cover changes are affected by the changes in the NPP and soil respiration and the effects of changing environmental conditions on these fluxes.

[18] Within a grid cell, cleared natural vegetation is replaced by croplands. With changes in natural vegetation, a specified amount of carbon is released from the three vegetation carbon pools (GV, NW, WTP) based on the relative proportions of the carbon contained in these reservoirs. A fraction of the released carbon is transferred to litter reservoirs as slash left on the ground. The rest is either released to the atmosphere by the burning of plant material to help clear the land for agriculture (Conversion Flux in Figure 1) or transferred to wood and/or fuel product reservoirs (Product Pools in Figure 1). The carbon added to the litter reservoir decays according to the decomposition rates of the litter reservoir as discussed earlier, and then carbon is released to the atmosphere. Carbon stored in the product reservoirs is released to the atmosphere at a variety of rates dependent on usage and assigned products into three general reservoirs with turnover times of 1 year (agriculture and agriculture products), 10 years (paper and paper products), and 100 years (lumber and long-lived products). We use the fractions of total cleared vegetation assigned to each product pool, vegetation amount burned and/or left as slash from *Houghton and Hackler* [2001], which varies with land cover type and region. We also assume that carbon is transferred from soil reservoirs to the litter reservoir. This carbon flux accounts for immediate carbon released due to soil cultivation following clearing and is assumed to be 25% of the carbon initially held in the DPM and RPM soil reservoirs [*Davidson and Ackerman*, 1993].

[19] In the case of croplands abandonment, the area of abandoned land is returned to the area of the pre-conversion natural vegetation type. Natural vegetation is then allowed to regrow from the extant state of the grid cell at the time of abandonment.

2.2. Data
2.2.1. Temperature, Precipitation, and Atmospheric CO_2 Data

[20] The monthly temperature and precipitation data used in this study is the CRU TS 2.0 observation data set of the Tydall Center (T. D. Mitchell et al., A comprehensive set of high-resolution grids of monthly climate for Europe and the globe: The observed record (1901–2000) and 16 scenarios (2001–2100), submitted to *Journal of Climate*, 2004). These climate data are available for the period 1900–2000, and the resolution of this data set is 0.5 degrees. For grid cells with missing data sets, particularly in the early twentieth century, relaxation to the climatology is applied to ensure the completeness of the data set in space and time. For initialization of the ISAM model back over the period between 1765 and 1899, we generated the climate data over this time period by randomly selecting yearly climate data between the period 1900 and 1920.

[21] Estimates of atmospheric CO_2 concentration from ice cores [*Neftel et al.*, 1985; *Friedli et al.*, 1986] and direct measurements given by *Keeling et al.* [1982] are specified from 1765 through 1958. The average of annual concentrations from the Mauna Loa (Hawaii) and South Pole Observatories [*Keeling and Whorf*, 2000] is specified for the period from 1959 through 1990.

2.2.2. Initial Natural Vegetation Distribution

[22] The global distributions for natural vegetation in 1765 (Figure 2) are estimated by superimposing the 1765 cropland data of *Ramankutty and Foley* [1999], and pastureland data of *Klein Goldewijk* [2001] over the potential vegetation data sets of *Ramankutty and Foley* [1999], which is primarily based on *Loveland and Belward* [1997] and *Haxeltine and Prentice* [1996] vegetation data sets. For the land cover changes starting in 1765, we superimpose the historical cropland data sets over the initial natural vegeta-

Table 2. Change in Regional and Global Area for Croplands Between 1765 and 1990, and 1980 and 1990 Based on HH and RF Data Sets[a]

	Area					
	1765–1990			1980–1989		
Regions	HH	RF	RF Percent Difference Relative to HH	HH	RF	RF Percent Difference Relative to HH
Tropical America	1.9	1.8	−5	0.33	0.03	−90
Tropical Africa	1.5	0.7	−53	0.41	0.09	−82
Tropical Asia	1.6	2.2	38	0.27	0.18	−40
Tropics total	5.0	4.7	−6	1.01	0.30	−70
North America	2.1	2.5	19	0.00	−0.07	...[b]
Europe	0.5	0.6	20	−0.03	−0.02	−33
North Africa and Middle East	0.8	0.5	−37	0.07	0.03	−57
Former Soviet Union	1.7	2.7	59	−0.02	−0.03	−78
China	0.8	1.1	29	0.00	−0.08	...[b]
Pacific developed regions	0.7	0.4	−43	0.19	0.02	−33
Nontropics total	6.6	7.8	15	0.21	−0.15	...[b]
Global	11.6	12.4	7	1.21	0.15	−88

[a]Unit of measure is million km^2. HH, *Houghton and Hackler* [1999, 2001] and *Houghton* [1999, 2000, 2003]; RF, *Ramankutty and Foley* [1998, 1999].

[b]Either HH value is zero or HH and RF have different signs. In this situation it is not appropriate to calculate the percentage difference.

tion data set. In the case of HH data set, it was necessary to adjust the areas for some of the natural vegetations in the 1765 when the rates of clearing for croplands required more land area than was available. The total initial adjusted area is very small (about 1.5%), and the effects of these minor adjustments on the final results should be small relative to the effects analyzed in this study.

2.2.3. Land Use Change Data

[23] Over the period 1765–1990, we calculated historical land use and net terrestrial biospheric carbon fluxes due to changes in land covers and abandonment based on *Houghton and Hackler* [1999, 2001], *Houghton* [1999, 2000, 2003] (HH), and *Ramankutty and Foley* [1998, 1999] (RF) data sets.

2.2.3.1. RF Data Set

[24] The RF data set provides geographically explicit changes in global croplands from 1700 to 1992. It was derived from spatially explicit maps of historical croplands using a satellite based 1992 cropland data [*Loveland and Belward*, 1997], and historical cropland inventory data compiled from various sources [*Ramankutty and Foley*, 1998, 1999], along with a simple land cover change model. RF estimates represent the extent to which different natural vegetation types have been converted to croplands and which cropland areas have been abandoned over the historical time period. However, they did not include other forms of land use change activities, such as clearing of forests for pastures and wood harvest. Their study provides the fractional areas for croplands and natural vegetation data for each 0.5° grid cell between 1700 and 1992. In this study we calculate yearly area weighted carbon fluxes for each vegetation type within each grid cell. Each year the fractional croplands and natural vegetation areas could increase or decrease within each grid cell, depending upon the land use change activities (clearing for croplands or abandonment) occurring within that grid cell. However, total area within each grid cell remains conserved.

2.2.3.2. HH Data Set

[25] HH estimated the yearly rates of land cover changes for croplands for nine regions (Table 2). The rates of land use change within each region are based on variety of sources. For the 1980s, the rates are primarily based on the deforestation rates compiled from the national reports and remote sensing surveys from the United Nations FAO (Food and Agriculture Organization) Forest Resource Assessment (FRA). Between 1961 and 1980, HH data are compiled based on the FAO Production Yearbooks. Prior to 1961, the HH data was compiled from the several global summaries of cropland areas through time [*Houghton et al.*, 1983, and references therein]. The estimates of HH provide the regional details of deforestation and abandonment of croplands, pasturelands, and the wood harvest by land cover type rather than by geographical details, as is the case with the RF data set. In this study we consider land cover changes for croplands and pasturelands only. In order to calculate land use emissions at a 0.5° grid scale, we distribute their regional rates of change by area weighted averaging within each grid cell of the land cover type converted for the cropland.

[26] Let ARC (i, k) be the regional area change (m^2) for vegetation type k into croplands within region i; TRA(i, k) is the total area of vegetation type k for region i, and GA(i, j, k) is the area of the jth grid cell of land cover type k within region i. Then the area change is

$$AGC(i,j,k) = ARC(i,k)\left(\frac{GA(i,j,k)}{TRA(i,k)}\right),$$

where

$$TRA(i,k) = \sum_{j=1}^{j=n} GA(i,j,k)$$

and n is the total number of grid cells of vegetation type k within region i.

[27] We used their positive deforestation rates to estimate rates of clearing and their negative rates to estimate rates of abandonment. We linearly interpolated the decadal rates of HH to obtain annual rates where necessary.

2.3. Model Steady State Simulations and Transient Experiments

2.3.1. Initial Steady State Simulation

[28] When analyzing the impact of climate change, it is important that the model be in equilibrium with climate conditions at the beginning of the simulation year 1765. This is due to the long turnover times of soil humus, which can make size of the equilibrium model reservoirs quite sensitive to the conditions assumed for generating the initial states [*Post et al.*, 1997]. Therefore we first ran the vegetation model with a 1765 atmospheric CO_2 concentration of 278 ppmv to calculate the equilibrium NPP and vegetation carbon. Then we initialized the soil carbon turnover model using the equilibrium litter inputs in two phases. First, we equilibrated the model with constant monthly mean climate of temperature and precipitation for the period 1900–1990. We selected the time period of 1900–1990 to account for the longest period of the fossil fuel era for which sufficient climate data are available for spatial interpolation. Since the soil component of the terrestrial biosphere at any given time would have experienced interannual variability in climate and not simply a mean climate, we continued the initialization process through 10 repetitions of the detrended monthly climate time series for the period 1900–1990. The climate time series was detrended for each month and for each grid cell using simple linear regressions to remove any long-term changes in climate. There is enough nonlinearity in the soil carbon components with respect to temperature and precipitation that the addition of these year-to-year variations in climate causes the soil carbon pools to drift downward to a new equilibrium.

2.3.2. Transient Simulations

[29] After running the model to equilibrium in 1765, we performed transient experiments through 1990. To estimate the marginal effects of increasing CO_2, climate change, and land cover changes for croplands on the terrestrial carbon cycle during the historical time period, we performed four experiments using our ISAM model. In the first experiment, E1, atmospheric CO_2 and climate were varied over the historical time period. In experiment E2, atmospheric CO_2 and land cover changes for cropland were varied. In experiment E3, atmospheric CO_2, climate, and land cover changes for cropland were varied. The land use emissions due to land cover changes for croplands were estimated by subtracting E1 from E3, and the effect of climate change was determined by subtracting E2 from E3. The marginal effect of increasing CO_2 was determined by subtracting the land use emission and climate change effects from experiment E3. In order to directly compare our model results with HH's bookkeeping model (that keeps track of carbon stocks and fluxes due to land cover changes only), we carried out an additional experiment, E4, where only land cover changes for cropland were varied over a historical time period.

This experiment does not account for temporal variations in CO_2 and climate.

3. Results

3.1. Steady State Results

[30] The ISAM estimated steady state global NPP and global total carbon for the 1765 climate and an atmospheric CO_2 concentration of 278 ppm were about 59 Gt C/yr and 2432 GtC (Table 1), respectively. Of this total carbon (TC), 35% (838 GtC) is stored as vegetation carbon (VC), and 65% (1594 GtC) as soil organic carbon (SOC). The model estimated NPP, VC, and SOC values fall within the range of other estimates at 45–61 GtC/yr [*Prentice et al.*, 2001; *Cramer et al.*, 1999; *Melillo et al.*, 1993], 500–950 GtC [*Eswaren et al.*, 1993; *Post et al.*, 1997], and 1500–1600 GtC/yr, respectively [*Post et al.*, 1982; *Eswaren et al.*, 1993; *Batjes*, 1996; *Jobbagy and Jackson*, 2000].

[31] Tropical evergreen is the most productive land-cover type and alone accounts for about 23% (13.7 GtC) of the global NPP and 32% (268 GtC) of VC storage. Other major productive land cover types are savanna, boreal forests, and tropical deciduous, which account for an additional 16% (9.7 GtC), 11% (6.4 GtC), and 10% (6.0 GtC) of total NPP, respectively. On the other hand, boreal forests store the maximum amount, 496 GtC (33%), of the SOC, followed by savanna (16%), and tundra (12%). Other land cover types store less than 10% of the global total carbon. Boreal forests also store the maximum amount of global TC (27%), followed by tropical forest (16%), and savanna (10%). Other land cover types store less than 10% of the global total carbon. Together, tropical evergreen, boreal forests, and savanna accounts for 53% of the global total terrestrial carbon storage. In terms of the percent of TC across the land cover types, 60–75% of the tropical and temperate forest carbon is stored in the forest vegetation, whereas most of the grassland (94%), shrublands (92%), and croplands (72%) carbon stocks are in soil. These differences in partitioning of TC between VC and SOC are likely to influence changes in global terrestrial carbon storage as these carbon reservoirs respond differently to changes in climate and atmospheric CO_2.

3.2. Transient Simulation Results

[32] This section presents the ISAM estimated global and annual mean changes in the NPP and terrestrial ecosystem carbon from 1765 to 1990 using the observed historical atmospheric CO_2 data and historical climate change data (precipitation and temperature data) based on reconstructed climate data from 1765 to 1899 and based on observation data from 1900 to1990. We also used HH and RF croplands data sets, which are compared below, to simulate the effects of land cover changes for croplands between 1900 and 1990. The experiments performed based on HH and RF data sets are defined here as ISAM-HH and ISAM-RF, respectively. In the following, first we compare HH and RF's cropland data sets.

3.2.1. Cropland Changes

[33] Figure 3 shows the geographic distributions of croplands based on two data sets for 1990. The hot spot areas for
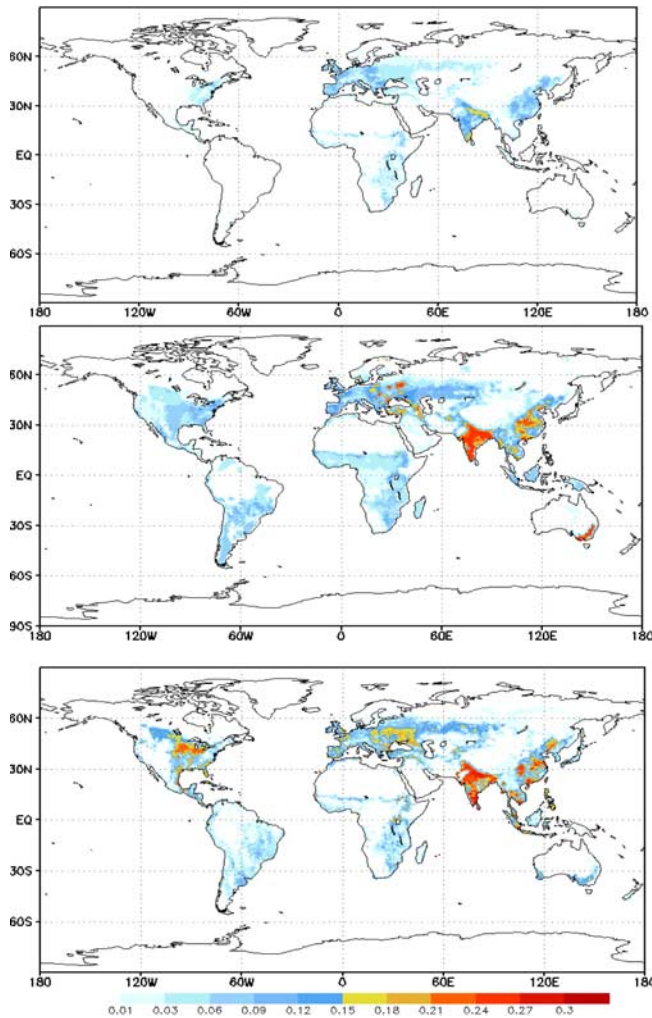
Figure 3. Spatial distribution of croplands (million km²) for years (top) 1765, (middle) 1990 based on *Houghton and Hackler* [1999, 2001] and *Houghton* [1999, 2000, 2003] data, and (bottom) 1990 based on *Ramankutty and Foley*'s [1998, 1999] data. The year 1765 cropland distribution is common for both data sets.

croplands shown in Figure 3 reveal a similar overall pattern for both data sets. Many dense agricultural areas exist in tropical Asia, China, central and eastern United States, southern Canada, Europe, western former Soviet Union, central and southern Latin America, and tropical Africa. Cropland areas are largely absent in extremely dry or cold regions within subtropical desert and high alpine regions and high latitude zones. The HH data show the homogeneous distribution of the cropland areas within a region because the rates of area changes are given in regional units, whereas cropland areas based on RF are in more geographic detail as they are based on gridded satellite and land cover imagery data sets.

[34] Table 2 compares HH and RF estimated net area change for croplands across nine major regions. Both data sets indicate that the total area of croplands have increased by about 12 million km² over the period 1765–1990. However, the RF based regional areas for cropland are up

to 59% greater than those estimated by HH. For the period 1765–1990, expansion of cropland areas based on RF is lower than HH estimates for tropical Africa (53%), North Africa, and the Middle East (37%), Pacific developed regions (43%), and Latin America (5%); whereas they are higher for the former Soviet Union (59%), tropical Asia (38%), China (29%), North America (19%), and Europe (EU, 20%) (Table 2). The expansion of croplands based on RF in the tropics was slightly lower (6%) than expansion based on HH data set, while in the nontropics it was higher (15%).

[35] For the 1980s decade, there is significant disagreement between the two data sets for the cropland areas. The differences are not only in the regional estimates but also in the global estimates. For this decade, the RF change in estimated global area for cropland is 0.2 million km², about 88% lower than the HH change in estimated value of 1.2 million km² (Figure 4 and Table 2). As for the regional estimates, RF change in estimated cropland areas for all regions are lower than HH estimates. In the case of tropical America, RF change in estimated cropland area is 90% lower than the HH estimates, which is the largest relative difference. The largest absolute difference is in tropical Africa where RF change in estimated croplands area is 0.09 million km² compared to HH estimated cropland area of 0.41 million km². HH estimates show no expansion occurring in China during the decade of 1980s. However, some studies have shown that official statistics in China may be underreporting agricultural land area by as much as 50%; correction for this fact would further increase the HH/RF discrepancy in cropland extent [*Ramankutty et al.*, 2002]. In the tropics, the cropland area based on the RF data set was about 70% lower than the HH data set. On the other hand, in the nontropical regions, cropland area was abandoned based on RF data, whereas HH data report the expansion of cropland area during the 1980s.

3.2.2. NPP, Vegetation, Soil Organic, and Total Carbon

[36] Table 3 shows the ISAM estimated relative percentage changes in NPP (GtC/yr), vegetation carbon (VC), and
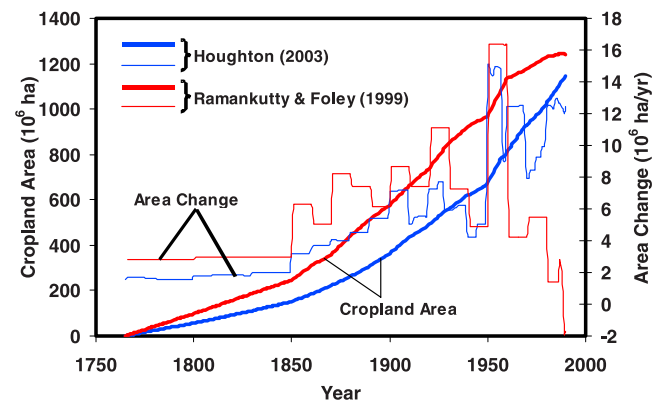

Figure 4. Global mean cropland areas and rates of changes based on HH [*Houghton and Hackler*, 1999, 2001; *Houghton*, 1999, 2000, 2003] and RF [*Ramankutty and Foley*, 1998, 1999] data sets.

Table 3. ISAM Model Estimated Percent Change During the 1765–1990 Period in NPP, Vegetation Carbon, Soil Organic Carbon, and Total Carbon Based on HH and RF Data Sets for Land Cover Changes for Croplands[a]

Land Cover Type	Net Primary Productivity (NPP)		Vegetation Carbon (VC)		Soil Organic Carbon (SOC)		Total Carbon (TC)	
	ISAM-HH	ISAM-RF	ISAM-HH	ISAM-RF	ISAM-HH	ISAM-RF	ISAM-HH	ISAM-RF
Tropical evergreen	2.5	2.1	−2.2	−3.2	−3.5	−4.2	−1.3	−3.2
Tropical deciduous	−11.0	−2.7	−14.9	−7.5	−16.9	−15.9	−15.5	−9.5
Temperate evergreen	−4.1	−13.3	−6.7	−18.4	−12.0	−23.2	−8.8	−20.5
Temperate deciduous	−21.8	−6.6	−23.7	−10.5	−24.0	−13.2	−23.8	−16.6
Boreal	3.9	−2.2	2.4	−4.4	1.1	−0.7	1.3	−1.5
Savanna	2.7	−0.7	1.7	−2.1	−27.6	−20.4	−24.6	−18.8
Grassland	−8.5	5.3	−9.1	4.5	−31.3	−15.4	−29.9	−13.9
Shrubland	13.8	8.7	12.6	7.2	6.4	−2.4	7.0	−1.5
Tundra	6.7	5.8	6.4	5.5	2.0	1.4	2.1	1.5
Desert	18.6	21.1	15.8	18.3	8.5	7.6	9.4	8.9
Polar ice/desert	0.0	0.0	0.0	0.0	6.0	52.5	6.0	52.5
Cropland	144.8	162.4	134.7	154.8	352.5	396.7	297.1	329.0
Pastureland	19.0	8.0	14.9	3.0	1.2	2.0	4.4	2.4
Total	7.0	8.5	−3.7	−3.8	2.3	2.0	0.3	0.0

[a]Abbreviations are as follows: HH, *Houghton and Hackler* [1999, 2001] and *Houghton* [1999, 2000, 2003]; RF, *Ramankutty and Foley* [1998, 1999]. The values are percent change in 1990 relative to 1765 values given in Table 1. ISAM-HH and ISAM-RF represent ISAM results based on HH and RF data sets, respectively.

soil organic carbon (SOC) in GtC based on HH and RF cropland data sets from 1765 to 1990. The changes are given for experiment E3 (climate, CO_2 fertilization effects, and net land use sources) simulations results. It is interesting to note that the estimated magnitudes of the relative changes in VC and SOC are quite different between the two data sets as well as across land cover types, mainly because the land cover change histories and the amount of land cover cleared for croplands based on the HH and RF data sets are quite different. The loss of soil carbon in savanna and grasslands is substantially higher than in the forests biomes, because in these two vegetation types, soils contain most of carbon, whereas the forests carbon stocks are primarily in vegetation. Owing to the expansion of overall cropland area during the twentieth century, the greatest increase relative to the 1765 values is in croplands' NPP (145 to 162%), VC (135 to 155%), SOC (352 to 397%), and total carbon (297 to 392%) based on the two data sets.

[37] Anthropogenically influenced changes in NPP and VC are primarily the result of four compensating effects: (1) an increase of NPP and VC due to climate and CO_2 fertilization-enhanced productivity of plants, (2) a reduction of NPP and VC due to climate change-increased autotrophic respirations, (3) a loss of VC and NPP due to land cover changes for croplands, and (4) an increase of NPP and VC due to abandonment of agricultural land and subsequent regrowth of forests.

[38] The relative changes in NPP are much higher than the relative changes in VC, mainly because changes in NPP (GtC/yr) are immediate, whereas relative changes in VC (GtC) are influenced by collective response across ecosystem types with differences in turnover times. Across vegetation types, forest biomes (with the exception of tropical evergreen and boreal forests) show a decrease in NPP and VC, whereas other land cover types, with the exception of grassland, show an increase in NPP and VC because most of the grass carbon stocks are in the soil. In the case of tropical evergreen, NPP increases based on both data sets, but VC decreases. In the case of boreal forests, NPP and VC

increase for the HH case, whereas simulations based on the RF data set resulted in a decrease of NPP and VC. The results are reversed for grasslands. This might be due to the differences in the amount of area cleared for croplands based on the two data sets as discussed in section 3.2.1. With changes in climate, atmospheric CO_2, and land cover changes for croplands over the period 1765–1990, the global NPP increased by 7–9%, whereas global VC decreased by about 4% based on HH and RF data sets. It is important to note that the increase in NPP is mainly due to CO_2 fertilization effect. In the case of climate change, NPP is quite stable because the changes in climate produce offsetting affect in NPP and autotrophic respirations [*Ryan et al.*, 1996, 1997].

[39] Anthropogenically influenced changes in SOC are more complex functions than those of VC. The changes in SOC due to climate and atmospheric CO_2 are also the results of four offsetting effects: (1) an increase of SOC due to increased litter input to the soil by increased atmospheric CO_2 concentration, (2) a reduction of SOC due to an increased soil decomposition rate by climate effect, (3) a release of SOC into the atmosphere due to an increased soil decomposition rate as a result of land cover changes for croplands, and (4) an increase of SOC due to abandonment of agriculture lands.

[40] With change in climate, atmospheric CO_2, and land cover changes for croplands, the relative change patterns across the ecosystem types are generally the same as in VC; however, across the land cover types, the relative loss of SOC was generally higher than the loss of VC. Globally, our model results show that SOC increased by about 2% based on HH and RF data sets by 1990.

[41] With the changes in climate, CO_2, and cropland land cover, TC declined in some ecosystems and increased in others (Table 3). Most forest ecosystems, savanna, and grasslands lost TC, while other ecosystem types, with the exception of shrublands, gained TC. In the case of shrublands, TC was gained based on HH data, whereas it lost TC based on the RF case. One important observation that we
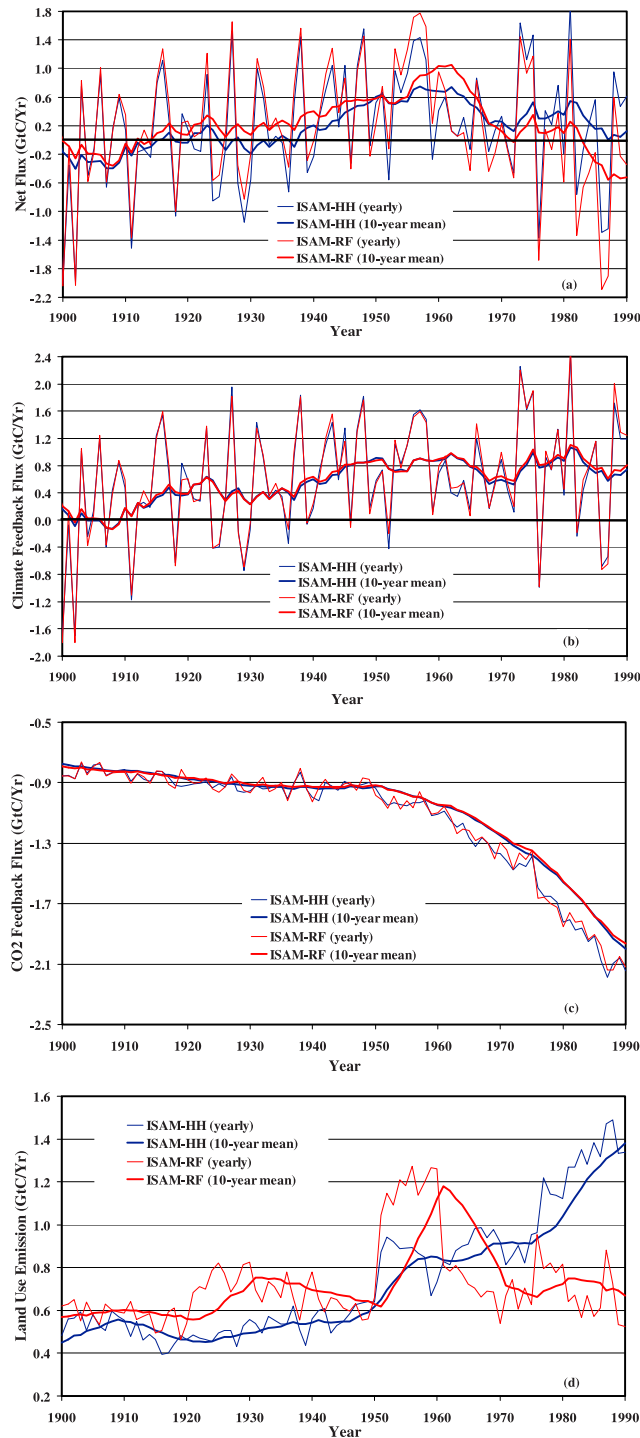
Figure 5. Partitioning of the yearly and 10-year running mean of ISAM estimated global and annual historical (a) net carbon exchange (GtC/yr) with atmosphere between 1900 and 1990 attributed to (b) climate change, (c) increase in CO_2 concentrations, and (d) cropland expansion and abandonment. Positive values represents net carbon release to the atmosphere and negative values represent net carbon storage in the terrestrial biosphere. The ISAM-HH and ISAM-RF results are based on Houghton's [*Houghton and Hackler*, 1999, 2001; *Houghton*, 1999, 2000, 2003], and *Ramankutty and Foley*'s [1998, 1999] data sets for cropland changes.

made in Table 3 is that all of the ecosystem types that lost/gained SOC actually lost/gained in TC. Globally, there was no change in TC in 1990 relative to 1765.

3.2.3.   Land Use Emissions and Net Land-Atmosphere Carbon Flux Associated With Changes in CO_2, Climate, and Croplands

3.2.3.1.   Land Use Emissions

[42] The land use emissions associated with changes in cropland is calculated by subtracting experiment E2 from experiment E3 as discussed in section 2.3.2. The ISAM model estimated carbon emissions (GtC/yr) for the period 1900–1990 derived based on HH and RF cropland changes data sets are shown in Figure 5d. The results reflect somewhat parallel images of the rate of changes in area for croplands shown in Figure 4. Both HH and RF data sets show a generally increasing rate of change of area for cropland until about 1960. Thereafter, both data sets reveal different trends until 1990. The RF data shows a sharp decrease in the rate of change in area for croplands between 1960 and 1990. In contrast, data based on HH shows first a decreasing trend between 1950 and 1970, then an increasing trend through the 1980s, even though HH based cropland changes stabilize or decrease during the late 1980s. This is due to the fact that emissions rates do not immediately follow the rates of changes for croplands; rather emission rates depend on the amounts and turnover rates of the product pools (i.e., forest products have slower turnover rates relative to agriculture and paper products, so forest products release emissions over longer timescales).

[43] In general, model results show substantial regrowth activities on the abandoned agriculture land for both data set cases, particularly north of the tropics (Figures 6a and 6b). Moreover, model results based on both data sets show substantial deforestation activities in tropical regions during the 1980s (Figures 6 and 7d). The simulation based on both data sets indicates that the combined nontropical, as well as Europe and former Soviet Union, land use component was approximately neutral during the 1980s (Figures 6 and 7d), because the effects of carbon storage associated with forest regrowth are approximately balanced by releases associated with the decomposition of agriculture, paper, and wood products. The model results also show large differences in the regional land use activities based on the two data sets. For example, results based on the RF data set shows the forest regrowth in eastern China and the United States, whereas these regions released substantial amount of CO_2 based on HH data set (Figures 6 and 7d). Moreover, in some regions, clearing for cropland-related emissions based on the RF data set was appreciably lower than HH based emissions during 1980s: 133% lower for North Africa and Middle East, 83% for tropical Africa, 80% for North America, 66% for Pacific developing regions, and 41% for tropical Asia, whereas in tropical America, emissions were 9% higher than the emissions based on the HH data set (Table 4). In absolute terms, the HH based land use emissions for tropical regions were substantially higher than the RF based emissions (Table 4). In terms of global results, the ISAM estimated land use emissions based on RF data for the 1980s are substantially lower than HH based estimates (50%) (Figure 7d and Table 4). In the next section,
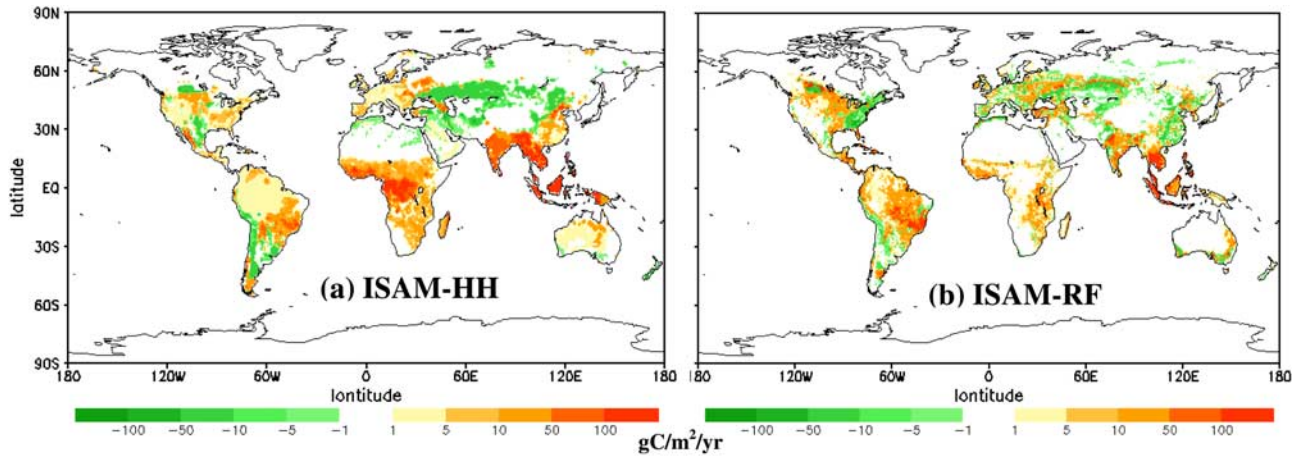
Figure 6. ISAM estimated spatial distributions of the mean net exchange of carbon (gC m^{-2} yr^{-1}) during the 1980s associated with cropland changes (E3 minus E1 case) based on (a) HH data [*Houghton and Hackler*, 1999, 2001; *Houghton*, 1999, 2000, 2003], and (b) RF [*Ramankutty and Foley*, 1998, 1999] cropland data sets. Positive values represent net carbon release to the atmosphere, and negative values represent net carbon storage in the terrestrial biosphere.

we explore the causes of differences in land use emissions estimates based on the two data sets.

3.2.3.2. Net Land-Atmosphere Carbon Flux

[44] Figure 5a compares ISAM estimated 10-year running mean and yearly net land-atmosphere fluxes of CO_2 (the sum of climate feedback fluxes (Figure 5b), CO_2 fertilization fluxes (Figure 5c), and CO_2 emissions associated with land cover changes (Figure 5d)) based on the HH and RF data sets between 1900 and 1990.

[45] First, it is important to recognize that the modeled net terrestrial CO_2 exchange with the atmosphere shows considerable interannual variability (Figure 5a), which is mainly induced by the interannual variations in climate feedback fluxes that are of the order of 1.0 GtC with occasional variations of almost 2.0 GtC (Figure 5b). On the other hand, the interannual variations in fertilization feedback fluxes are small (Figure 5c).

[46] Figure 5b shows that there was a net release of CO_2 from the terrestrial ecosystems to the atmosphere from 1900 to 1990, primarily as a consequence of increased rates of soil decomposition of current vegetation as a result of climate change. On the other hand, there was a continuous increase of CO_2 storage by the terrestrial ecosystems due to the fertilization effect over the period 1900–1990, primarily due to enhancement of plant productivity (Figure 5c). Overall, the storage of CO_2 due to CO_2 fertilization feedback is significantly higher (2.1 GtC/yr by 1990) as compared to the CO_2 release due to climate feedback (0.8 GtC by 1990).

Table 4. ISAM Estimated Land Use Emissions and Net Terrestrial Net Carbon Uptake Over the Periods 1765–1990 and 1980–1989 Based on HH and RF Data Sets[a]

| | Land Use Emission, GtC | | | | | | Net Terrestrial Carbon Emission, GtC | | | | | |
| | 1765–1990 | | | 1980–1989 | | | 1765–1990 | | | 1980–1989 | | |
Regions	ISAM-HH GtC	ISAM-RF GtC	Percent Change[b]	ISAM-HH GtC	ISAM-RF GtC	Percent Change[b]	ISAM-HH GtC	ISAM-RF GtC	Percent Change[b]	ISAM-HH GtC	ISAM-RF GtC	Percent Change[b]
Tropical America	13.6	14.9	10	2.2	2.4	9	−19.5	−16.5	−15	−1.0	−0.5	−50
Tropical Africa	16.0	4.8	−70	4.8	0.8	−83	−0.9	−13.0	44	0.7	−3.3	...[c]
Tropical Asia	32	34.7	8	5.8	3.4	−41	20.2	23.2	15	3.9	1.4	−64
Tropics	61.5	54.3	−12	12.8	6.7	−48	−0.3	−6.3	21×	3.6	−2.4	...[c]
North America	16.6	22.3	34	0.5	0.1	−80	5.6	13.3	137	0.4	0.2	−50
Europe	4.5	6.2	38	0.1	0.0	...[c]	1.3	3.5	169	−0.5	−0.5	0
N. Africa & M. East	1.4	1.7	21	−0.3	0.1	−133	−2.1	−1.9	−9	−0.7	−0.4	−43
Former Soviet Union	7.7	16.1	109	−0.5	0.0	...[c]	−9.4	−1.1	−94	−0.1	0.8	...[c]
China	14.5	11.5	−20	0.2	−0.3	...[c]	6.3	2.9	−88	−0.8	−1.1	37
Pacific Developing	2.5	1.3	−48	0.3	0.1	−66	−7.6	−8.3	9	−1.5	−1.7	13
Non-Tropical Regions	47.1	59.1	25	0.5	0.0	...[c]	−5.8	8.4	...[c]	−3.2	−3.1	−3
Global	108.6	113.4	4	13.3	6.7	−50	−6.1	2.1	...[c]	0.4	−5.7	...[c]

[a]Abbreviations are as follows: HH, *Houghton and Hackler* [1999, 2001] and *Houghton* [1999, 2000, 2003]; RF, *Ramankutty and Foley* [1998, 1999]. Model also incorporates the effects of climate and increasing CO_2 concentrations for both data sets simulations. Positive values indicate net release to the atmosphere and negative values indicate net storage in the terrestrial biosphere.

[b]Change is relative to ISAM-HH.

[c]Either RF value is zero or HH and RF have different signs. In this situation it is not appropriate to calculate the percentage difference.
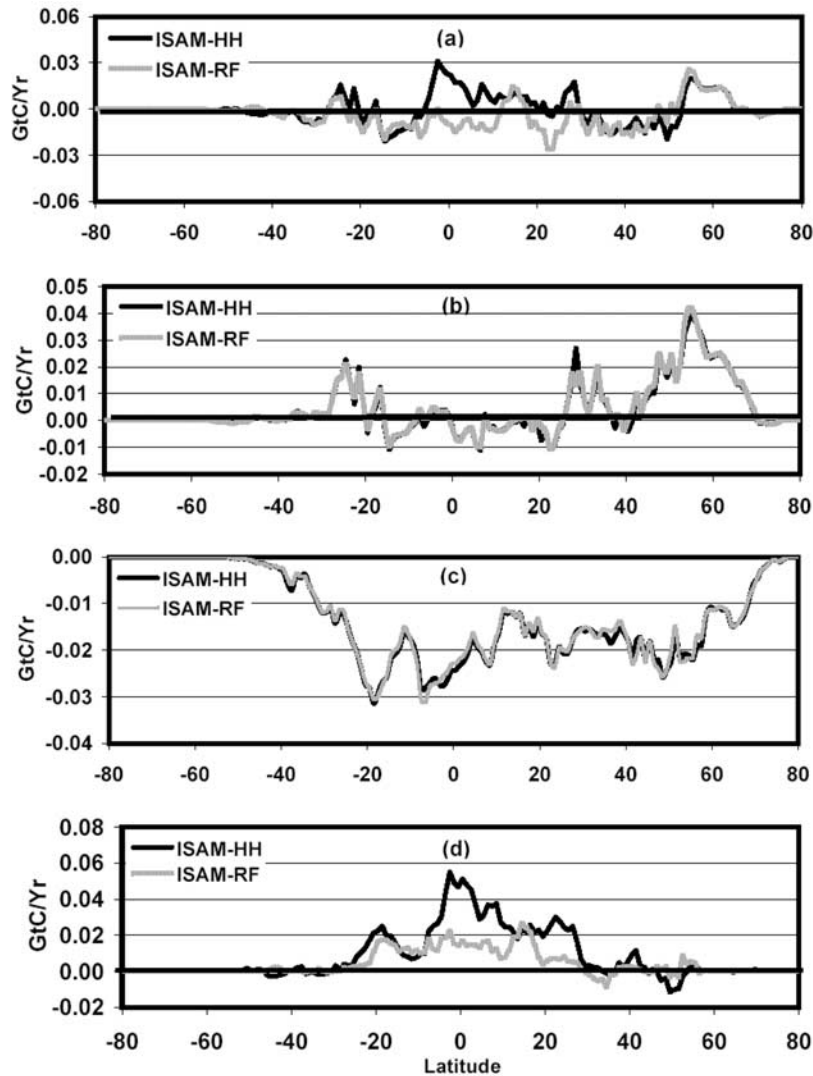
Figure 7. Partitioning of the ISAM estimated annual mean latitudinal distribution of (a) net ecosystem carbon (GtC/yr) attributed to changes in (b) climate, (c) increase in CO_2 concentrations, and (d) cropland expansion and abandonment. The results are compared for HH data [*Houghton and Hackler*, 1999, 2001; *Houghton*, 1999, 2000, 2003], and RF [*Ramankutty and Foley*, 1998, 1999] cropland data cases for the 1980s. Positive values represents net carbon release to the atmosphere, and negative values represent net carbon storage in the terrestrial biosphere.

[47] Figure 5a shows that from around 1900 to 1990, there were substantial differences in the net land-atmosphere fluxes calculated based on the HH and RF data sets. For the period 1900–1910, our model results show that terrestrial ecosystems acted as a sink for atmospheric CO_2 for both data sets. Thereafter the results based on the RF data set show that the terrestrial ecosystems gradually become a source whereas the net flux calculated based on the HH data set fluctuate between −0.2 and 0.2 GtC/yr up until 1938 and then the flux gradually increases. The results based on both data sets show that the amounts of CO_2 released into the atmosphere peaked around 1962 and start declining thereafter. However, the estimated fluxes determined from the RF data between 1900 and 1968 are slightly greater than fluxes determined from the HH data and vice versa thereafter. Overall, ISAM estimated net land-atmosphere flux based on the HH data set between 1765 and 1990 was −0.6 GtC/yr as compared to RF data-based estimated flux of −0.2 GtC/yr.

[48] The differences are particularly pronounced in the 1980s, when fluxes based on both data sets begin declining (Figure 5a). However, the decline based on RF data was much steeper than HH data set. The model results indicate that these large differences are mainly due to the differences in the estimated net biospheric CO_2 uptake in the tropics based on the two data sets during the 1980s (Figure 7a). In general, the model in the tropics simulates net sink activity based on RF data and source activities based on HH data (Figures 7a and 8). The results based on both data sets indicate that the terrestrial biosphere was a sink of atmo-
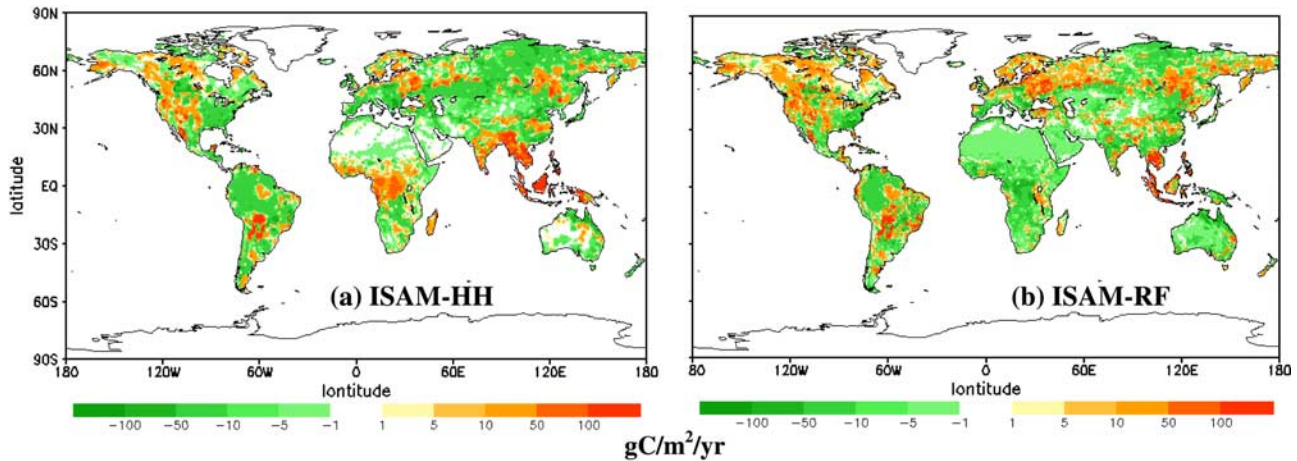
Figure 8. ISAM estimated spatial distributions of the mean net exchange of carbon (gC m^{-2} yr^{-1}) during the 1980s associated with climate, CO_2 increase, and cropland changes based on (a) HH data [*Houghton and Hackler*, 1999, 2001; *Houghton*, 1999, 2000, 2003], and (b) RF [*Ramankutty and Foley*, 1998, 1999] cropland data sets. Positive values represent net carbon release to the atmosphere, and negative values represent net carbon storage in the terrestrial biosphere.

spheric CO_2 in the midlatitudes (Figures 7a and 8). However, in spite of much smaller land use fluxes in northern high latitudes (Figures 6 and 7d), particularly between 45°N and 70°N, the model simulates net source activities based on both data sets, because the estimated climate related carbon released to the atmosphere is much higher (Figure 7b) than the CO_2 fertilization related carbon sink (Figure 7c).

[49] Most importantly, model results for the 1980s derived from the RF data set demonstrate the terrestrial biosphere acting as a sink of atmospheric CO_2 (-0.57 GtC/yr) while those derived from the HH data set demonstrate the biosphere acting as a source (0.04 GtC/yr) (Table 4). Since the climate and CO_2 related terrestrial fluxes during the 1980s are approximately the same based on two data sets (Figures 7b and 7c), the differences in net fluxes are mainly due to differences in the estimated net land use sources based on the two data sets (Figure 7d). In the following, we examine the causes of differences in the land use emissions based on HH and RF data sets.

3.2.4. Examining the Causes of Differences in the Estimated Land Use Emissions

[50] Various hypotheses have been proposed for the causes of the differences in land use emission estimates based on HH and RF data sets. For example, *McGuire et al.* [2001] argued that their estimated land use fluxes for the 1980s might be lower than *Houghton*'s [1999] bookkeeping estimates because *Houghton* [1999] not only considered changes in croplands but also in pasturelands, shifting cultivation and wood harvesting [*McGuire et al.*, 2001]. *House et al.* [2003] proposed that in addition to the pastureland, differences in land use emissions based on *Houghton* [2003] and *McGuire et al.* [2001] estimates might be due to the differences in the modeling framework used, and differences in the vegetation types (forest versus grasslands) cleared during the cropland expansion. Here we reexamine the validity of some of these arguments using our ISAM.

3.2.4.1. Process Based Model Versus Bookkeeping Model

[51] One of the major differences between CCMLP's process based models and *Houghton*'s [1999] bookkeeping model is that the booking model does not account for biospheric response to climate and atmospheric CO_2, whereas processes based models do account for such effects. However, the *McGuire et al.* [2001] study concluded that the differences between the land use fluxes estimated by booking and process-based models could not be due to the climate and CO_2 fertilization effects. McGuire et al. found very little difference between the land use only case (equivalent to ISAM-RF(E4) case here) and the case where sources account for the effect of rising CO_2 and climate change (ISAM-RF case here). They argued that although the carbon storage associated with increasing CO_2 is enhanced in the regrowing forests in E3 simulation, this enhanced carbon storage is compensated by enhanced carbon release associated with land cover changes based on RF data. It is important to note that for the RF data case we also found little difference between land use only (ISAM-RF(E4)) case and base case (ISAM-RF) over the entire period 1900–1990 (Figure 9a), and in particular for the 1980s. We draw a similar conclusion in the case of HH data case. The emissions in the case of ISAM-HH case are slightly higher than ISAM-HH(E4), particularly during the 1980s, but such small differences cannot explain the large differences in the net release of CO_2 based on HH and RF data sets.

[52] There could be many other minor differences between the process and bookkeeping models. However, our modeling results do not support the suggestion that divergence between the *McGuire et al.* [2001] and *Houghton* [2003] results could be due to such differences in modeling framework. ISAM modeling framework and CCMLP models used similar methods to simulate ecosystem dynamics, and used *Houghton et al.*'s [1983] approach to estimate the product fluxes. The ISAM was able to capture the main
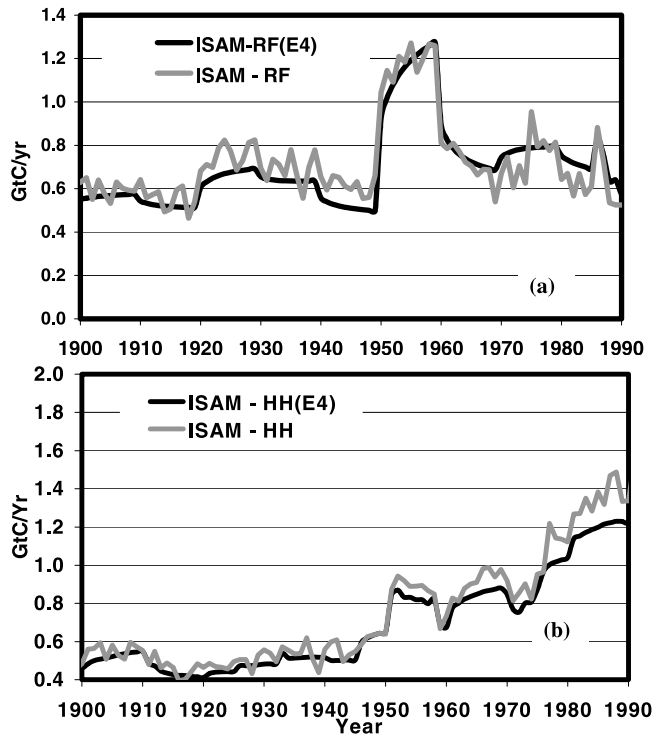
Figure 9. ISAM estimated global and annual mean net CO_2 release in the atmosphere land use emissions between 1900 and 1990 associated with land cover changes for croplands only case (E4 case), and for the standard case (E3 minus E1 case) where CO_2 release is estimated by subtracting the simulation that consider increasing atmospheric CO_2 and climate change (E1 case) from that of a simulation that consider cropland changes in addition to increasing atmospheric CO_2 and climate change (E3 case). The calculations were carried out using cropland changes data based on (a) RF [*Ramankutty and Foley*, 1998, 1999], and (b) HH [*Houghton and Hackler*, 1999, 2001; *Houghton*, 1999, 2000, 2003].

features of Houghton's (equivalent to ISAM-HH(E4) case here) and CCMLP models' (equivalent to ISAM-RF case here) estimated land use fluxes for cropland changes. If the differences had been due to differences in the modeling framework, our model would not have been able to capture the important features of both studies at the same time.

3.2.4.2. Pasturelands Versus No Pasturelands

[53] While changes in area for croplands have been the dominant source of land use emissions for CO_2 since preindustrial time, there are other land use change activities, such as pasturelands [*Houghton*, 2003] that may likely lead to higher land use emissions. According to *Houghton* [2003], pasturelands activities were responsible for about 15% of the total land use emissions in 1980s. *House et al.* [2003] and *McGuire et al.* [2001] hypothesized that the higher land use emissions based on the HH data set might be due the fact that bookkeeping model results using HH data set of *Houghton* [2003] not only incorporated land use emissions due to cropland changes but also pastureland

changes. However, our modeling results do not support suggestions that differences between *McGuire et al.* [2001] and *Houghton* [2003] land use emissions stem from the omission of pastureland changes by *McGuire et al.* [2001]. As Figure 5d shows, the divergence in the estimated land use emissions based on HH and RF data sets during the 1980s remain large even without incorporation of the pastureland change activities.

3.2.4.3. Grassland Conversion Versus Forest Conversion

[54] *House et al.* [2003] suggest that due to the spatially explicit nature of the cropland data used by CCMLP models, they may assume conversion of grasslands to croplands in regions where *Houghton* [2003] may have assumed forest conversion, especially in tropical Africa where the biggest differences between the HH and RF data sets are found. Contrary to the House et al. assertion, analysis of HH and RF cropland data sets for the tropical Africa region over the 1950–1990 period show that about one third of the crop covers came from forests in both data sets, while two thirds came from savanna/grasslands. The FAO based HH data set assumed that during the 1980s about 35% of the crop covers in tropical Africa come from the closed forest and the rest come from savanna/grasslands. In contrast, the RF data set assumes that 15% of the crop covers come from the tropical evergreen, 16% from tropical deciduous, and the rest from savanna/grasslands/shrublands. In order to further explore this issue, we assume that only 15% of the crops come from tropical forests instead of 35% as in the original HH data set, 16% from tropical deciduous, and the rest from savanna/grasslands. These changes are assumed to occur after 1950, because RF data for tropical Africa prior to 1950 is consistent with HH data for cropland changes [*Ramankutty and Foley*, 1999]. We define this modified case for tropical Africa as ISAM-HH(MTA). For all other regions, cropland changes are assumed to be the same as in the standard case (ISAM-HH). Figure 10 shows that our estimated land use emissions for the MTA case are slightly lower than the ISAM-HH case, nearly 8% lower in the 1980s and 10% in the 1990s. However, we believe that these differences are relatively small and probably do not solely explain the gap between *McGuire et al.* [2001] and *Houghton* [2003] for land use emissions. We believe the differences in the tropical Africa emissions based on *McGuire et al.* [2001] and *Houghton* [2003] results are due to the differences in total area cleared for croplands based on HH and RF data sets (Table 2). According to RF data, a 0.7 million km^2 area of natural vegetation type was converted for croplands over the 1765–1990 period, which was more than 50% lower relative to the HH data set (Table 2).

3.2.4.4. Spatially Explicit Versus Regionally Explicit Cropland Data

[55] In order to further investigate the reasons for the differences, we tested one of the assumptions we made regarding the distribution of *Houghton*'s [2003] regionally resolved land cover change data for cropland changes. To date, most of the carbon cycle modeling studies using Houghton's deforestation rates based on historical land use emission data are either done using simple schematic
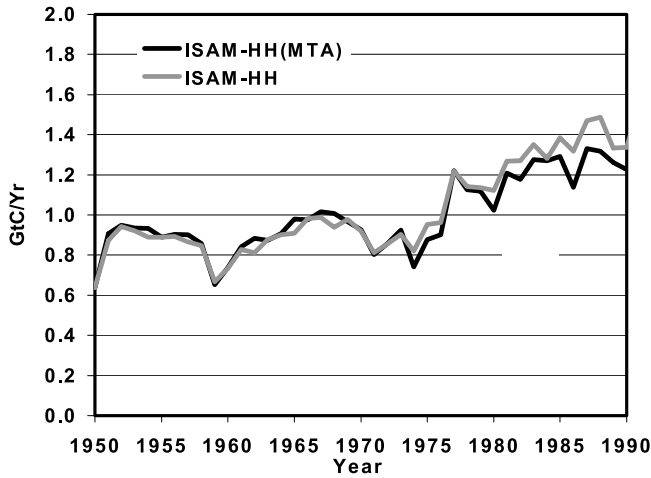
Figure 10. ISAM model estimated net atmospheric CO_2 release between 1900 and 2000 based on HH's cropland data [*Houghton and Hackler*, 1999, 2001; *Houghton*, 1999, 2000, 2003] (ISAM-HH case) and modified data for tropical Africa (ISAM-HH(MTA)) as discussed in the text.

models [e.g., *Enting et al.*, 1994; *Prentice et al.*, 2001; *Kheshgi and Jain*, 2003] or regional models [*Gitz and Ciais*, 2003]. To our knowledge, this is the first attempt to incorporate Houghton's regionally specific land cover change data into a spatially resolved terrestrial model. Houghton's data assign the rates of change (clearing or abandonment) for croplands to specific ecosystem types within nine regions. Since the data are not spatially explicit, we allocate the changes by area-weighted averaging over all 0.5° points of cleared ecosystem within each region as discussed in section 2.2.3. This approach does not consider

the spatially resolved cropland expansion. It only considers the area-weighted average cropland expansion across each specific land cover type within a region. This approach may assume expansion of cropland in places where it might not have occurred. In order to test the validity of our assumption, we used spatially resolved RF data for cropland changes and redistributed the changes according to the area-weighted averaging (AWA) approach as used for the HH data distribution. We define this case as the ISAM-RF(AWA) case. The cropland area distribution is now somewhat homogeneous (Figure 11) due to the area-weighted averaging and looks similar to the HH data set (Figure 3, middle). Figure 12 shows that the model estimated land use emissions for the RF-averaging case are similar to the RF standard case over the period 1900–1990. Overall, the model-estimated emissions for the RF-averaging case for the 1980s were 0.71 GtC/yr compared to the RF standard case value of 0.64 GtC/yr. We believe the differences between these two land use emission trends to be insignificant relative to differences in the emission trends for the two data sets analyzed here. Moreover, these results suggest that land use emissions are not sensitive to the spatially explicit location of the natural vegetation converted to croplands within a region as long as the corrected ecosystems are converted. This may be due to the fact that the carbon amount and turnover rates of vegetation products are mostly functions of vegetation type, not functions of spatial variation. For example, forest products, in general, will have higher vegetation carbon storage and slower turnover rates, independent of location, as compared to grasslands or shrublands. Therefore we would expect higher emissions with time due to conversion of forests to croplands, as compared to conversion of grasslands or shrublands to cropland. Nevertheless, in some extreme cases, for example, if most productive area is converted for croplands
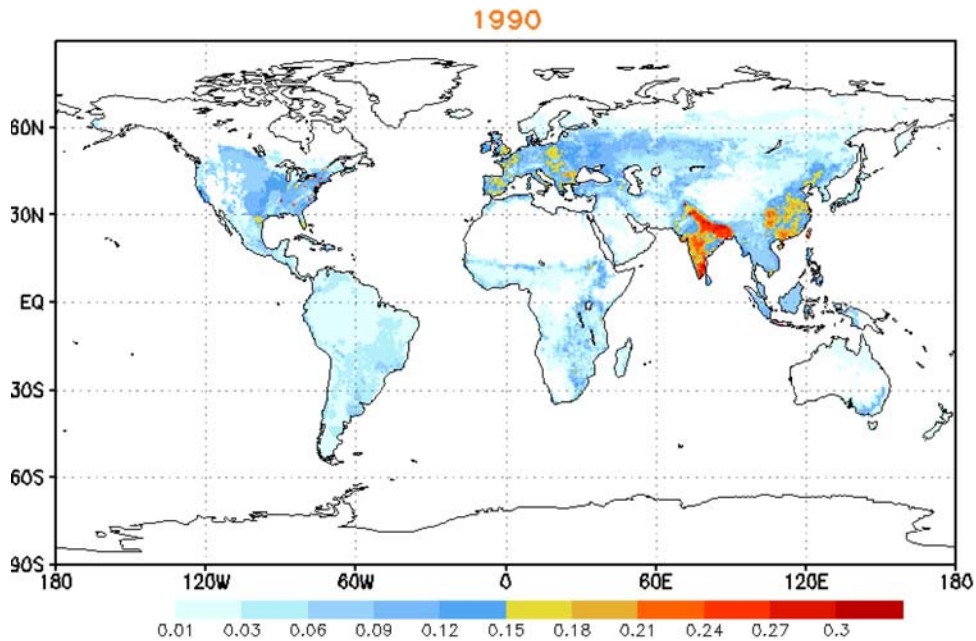

Figure 11. Redistribution of spatially resolved RF's [*Ramankutty and Foley*, 1998, 1999] (million km^2) cropland changes data using the area weighted averaging (AWA) approach.
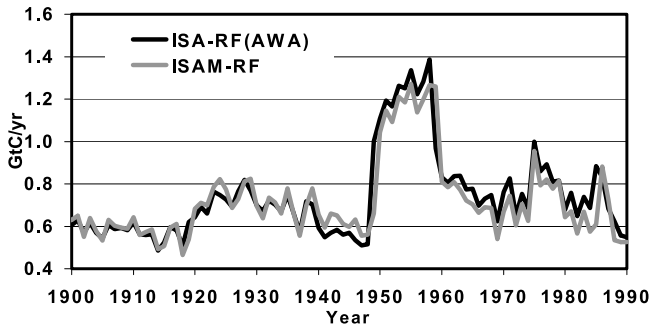
Figure 12. ISAM estimated net atmospheric CO_2 release between 1900 and 1990 for spatially resolved (ISAM-RF) and regionally resolved (ISAM-RF (AWA)) RF cropland data [*Ramankutty and Foley*, 1998, 1999] cases.

and least productive area is reverted, we would not expect the same outcome as we have found here.

[56] From the foregoing discussion and results based on our model we conclude that the differences between the two land use emissions for cropland changes can neither be modeling framework related nor pastureland emission or global land use practices related. The divergence between the two sets of land use fluxes is primarily due to the differences in the rates of changes in land area amount for croplands (Figure 4).

4. Comparing ISAM Estimates With Other Studies

[57] Our model-estimated mean annual latitudinal and global trends in the net carbon exchange with the atmosphere due to changes in CO_2, climate, and cropland

between 1980 and 1989 are compared in Tables 5 and 6 with the previous model studies by *McGuire et al.* [2001], *Houghton* [2003], and the IPCC [*Prentice et al.*, 2001]. ISAM model results for the ISAM−RF case are directly comparable with the *McGuire et al.* [2001] modeling study because both make use of the same land use change data set (RF), and both take into account the effects of climate and CO_2 increase, and are run on a $0.5°$ grid resolution. Similarly, when neglecting the influence of increasing atmospheric CO_2 and temperature (experiment E4), ISAM results for global and annual mean case are directly comparable to those of *Houghton* [2003].

4.1. Comparison With McGuire et al.

[58] Table 5 compares ISAM modeling results for the ISAM-RF case with the *McGuire et al.* [2001] model intercomparison study. At the global scale, both modeling studies suggest that the terrestrial ecosystems were a sink of atmospheric CO_2 during the 1980s. The ISAM estimated net terrestrial sink for the 1980s was -0.6 GtC/yr, which falls well within the range of values estimated by McGuire et al. (-1.3 to -0.3 GtC/yr). Both the modeling studies estimate a large contribution to CO_2 uptake from CO_2 fertilization during the 1980s (ISAM: -2.0 GtC/yr; McGuire et al: -3.2 to -0.9 GtC/yr), and a smaller contribution of biospheric CO_2 release due to the climate effect (ISAM: 0.7 GtC/yr; McGuire et al: -0.2 to 0.9 GtC/yr) (Table 5) compared to the CO_2 fertilization effect. The ISAM estimated land use emissions (0.7 GtC/yr) for the 1980s are also comparable to the McGuire et al. estimated values (0.6 to 1.0 GtC/yr).

[59] North of the tropics, both modeling studies predict net terrestrial sink during the 1980s. However, our model estimation (-0.2 GtC/yr) is at the lower end of the *McGuire et al.* [2001] range of values (-0.3 to -1.3 GtC/yr). This may be

Table 5. Comparing the ISAM Estimated Mean Annual Changes in the Terrestrial Carbon Flux (GtC/yr) Due to Climate, Increase in CO_2 Concentrations, and RF Based Land Use Changes for Croplands With *McGuire et al.* [2001] Between 1980 and 1989[a]

Region	Effect	ISAM-RF	*McGuire et al.* [2001]
Global	climate	0.7	−0.2 to 0.9
	CO_2	−2.0	−3.2 to −0.9
	land use	0.7	0.6 to 1.0
	total	−0.6	−1.5 to −0.3
30°N−90°N	climate	0.5	−0.1 to 0.4
	CO_2	−0.7	−1.6 to −0.2
	land use	0.0	−0.4 to 0.3
	total	−0.2	−0.3 to −1.3
30°N−30°S	climate	0.2	−0.1 to 0.7
	CO_2	−1.2	−1.4 to −0.6
	land use	0.7	0.5 to 1.2
	total	−0.3	−0.2 to 0.5
30°S−90°S	climate	0.0	0.0
	CO_2	−0.1	−0.1 to 0.0
	land use	0.0	0.0 to 0.3
	total	−0.1	0.0 to 0.2

[a]RF denotes *Ramankutty and Foley* [1998, 1999]. The results are compared for global ecosystems, north of 30°N, tropics, and south of 30°S. The total is a sum of all three effects: climate, increase in CO_2, and land use change. Positive values indicate net release to the atmosphere, and negative values indicate net storage in the terrestrial biosphere.

Table 6. Comparison of ISAM Estimated Annual and Global Mean Land Use Emissions and Net Land-Atmosphere Fluxes With *Houghton* [2003] and IPCC [*Prentice et al.*, 2001] for Various ISAM Cases During 1980s[a]

Study	Land Use Emissions	Net Land-Atmosphere Flux
This study		
ISAM − RF(E4)[b]	0.70	
ISAM − RF[c]	0.67	−0.57
ISAM − RF (C + P)[d]	1.60	0.43
ISAM − HH (E4)[b]	1.18	
ISAM − HH[c]	1.33	0.04
ISAM − HH (C + P)[d]	2.06	0.83
Overall range[e]	1.33 to 2.06	0.43 to 0.83
McGuire et al. [2001]	0.6 to 1.0	−1.5 to −0.3
Houghton [2003]		
Croplands	1.21	
Cropland + Other	1.98	
IPCC [*Prentice et al.*, 2001]	0.6−2.5	−0.9−0.5

[a]Units are GTC/yr.
[b]This does not consider the climate and changes in increasing CO_2 effects.
[c]This considers changes in climate, CO_2, and croplands.
[d]This considers changes in climate, CO_2, croplands, and pasturelands.
[e]The lower and higher range values are based on ISAM − RF (C + P) and ISAM − HH (C + P) cases values.
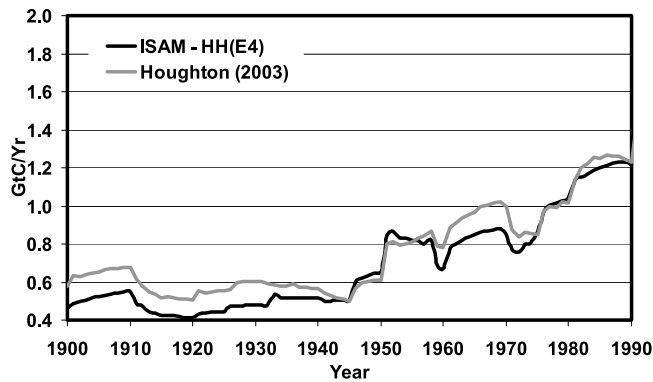
Figure 13. Comparison of *Houghton*'s [2003] bookkeeping model and ISAM model estimated global and annual mean net land use carbon fluxes (GtC/yr) between 1900 and 2000 for cropland changes only case (E4 case). Both model simulations are carried out using the cropland changes data from HH [*Houghton and Hackler*, 1999, 2001; *Houghton*, 1999, 2000, 2003].

due to the fact that ISAM estimates a slightly higher positive (0.5 GtC/yr) climate-carbon cycle feedback in the north of the tropics as compared to McGuire et al. estimates (−0.1 to 0.4 Gt/C) during the 1980s. The simulations by ISAM (0.0 GtC/yr) and McGuire et al. (−0.4 to 0.3 Gt/C) indicate that the land use emissions are approximately neutral in the north of the tropics because the release of carbon related to the land use clearing for cropland is apparently compensated by the sink associated with the forest regrowth.

[60] In the tropics, our model results indicate that the terrestrial biosphere was a sink (−0.3 GtC/yr) for atmospheric CO_2 during the 1980s. However, the model estimated net terrestrial sink is slightly higher than the results estimated by *McGuire et al.* [2001] (−0.2 to 0.5 GtC/yr). Nevertheless, our model estimated climate (0.1 GtC/yr), CO_2 (−1.2 GtC/yr) and land use (0.8 GtC/yr) effects are apparently within the range of values of McGuire et al. (climate: −0.1 to 0.7; CO_2: −1.4 to −0.6 GtC/yr; land use: 0.5 to 1.2 GtC).

[61] South of the tropic, the land area is small compared to the tropics and the north of tropic. Therefore ISAM and *McGuire et al.* [2001] models estimate small changes in the carbon flux of the terrestrial ecosystems. ISAM (−0.1 GtC/yr) and McGuire et al. (0.0 to 0.2) model studies indicate that south of tropics was approximately neutral during the 1980s.

4.2. Comparison With Houghton

[62] The ISAM model results are compared for the E4 experiment with cropland changes, neglecting temperature and atmospheric CO_2 feedback (much like the bookkeeping model of *Houghton* [2003], defined here as ISAM-HH(E4). For the period 1900–2000, Figure 13 compares the HH's bookkeeping model estimated land use fluxes for cropland changes only with our model response (GtC/yr) for ISAM-HH(E4). Since our estimates use the *Houghton* [2003]

cropland change history and many of the same assumptions for the product fluxes, our model results for E4 experiment are consistent with the *Houghton* [2003] bookkeeping model results. The two model results for land cover changes for cropland only cases do not differ by more than 0.13 GtC/yr during any time between 1900 and 2000. Our estimated emissions for the 1980s (1.18 GtC/yr) are consistent with *Houghton* [2003] estimates (1.21 GtC/yr). However, our model slightly underestimates the land use sources between 1900 and 1940 and during the 1960s. It should be noted that we use a dynamic model to describe the fate of carbon in disturbed ecosystems instead of the synoptic response functions used by *Houghton* [2003]. Moreover, natural ecosystems at equilibrium have different carbon contents in Houghton's model than we get with ours.

4.3. Comparison With IPCC

[63] The IPCC range of values for land use emissions for the 1980s is based on *Houghton* [1999, 2000], *Houghton and Hackler* [1999], and CCMLP model results [*McGuire et al.*, 2001], while the net land atmospheric flux was estimated from atmospheric measurements of CO_2 and O_2. Houghton's land use emission estimates not only account for land cover changes for croplands but also for pastureland, and wood harvest and shifting cultivation activities. Since the land cover changes for pasturelands are the second dominant source (after croplands) of land use emissions [*Houghton and Hackler*, 1999, 2001; *Houghton*, 1999, 2000, 2003] and *Houghton and Hackler* [1999, 2001] and *Houghton* [1999, 2000, 2003] also provide the pastureland change activities for the period 1765–1990, for this comparison we extend our model simulations for changes in area to pasturelands in addition to croplands. Because RF data do not provide the information for the historical pastureland changes, we incorporate the *Houghton and Hackler* [1999, 2001] and *Houghton* [1999, 2000, 2003] based historical pastureland changes not only in HH (defined here ISAM-HH(C + P) case) but also in RF cropland data sets (defined here ISAM-RF (C + P) case).

[64] Therefore we calculate the upper range of ISAM values for land use emissions and net land-atmosphere flux for 1980s by considering the effects of CO_2 and climate, and changes in area for pasturelands in addition to croplands. The pastureland change data for this study is taken from *Houghton* [2003]. The lower range of values is calculated in the same manner as CCMLP models calculated, that is by considering the land cover changes for croplands data taken from RF data set.

[65] As expected, the ISAM estimated combined land emissions scaled upward approximately the same amount in ISAM-HH(C + P) and ISAM-HH(C + P) cases (Figure 14b), whereas the estimated range of values for the net terrestrial uptake (sink) has become smaller than the cropland only case (Figure 14a). The ISAM estimated range of values for the pastureland changes in addition to croplands (lower and higher range of values are based on ISAM-RF(C + P) and ISAM-HH(C + P) cases, respectively) for land use emissions in the 1980s were 1.60 to 2.06 GtC/yr (1.83 GtC/yr was middle of the range value), whereas the estimated range of values for the net terrestrial
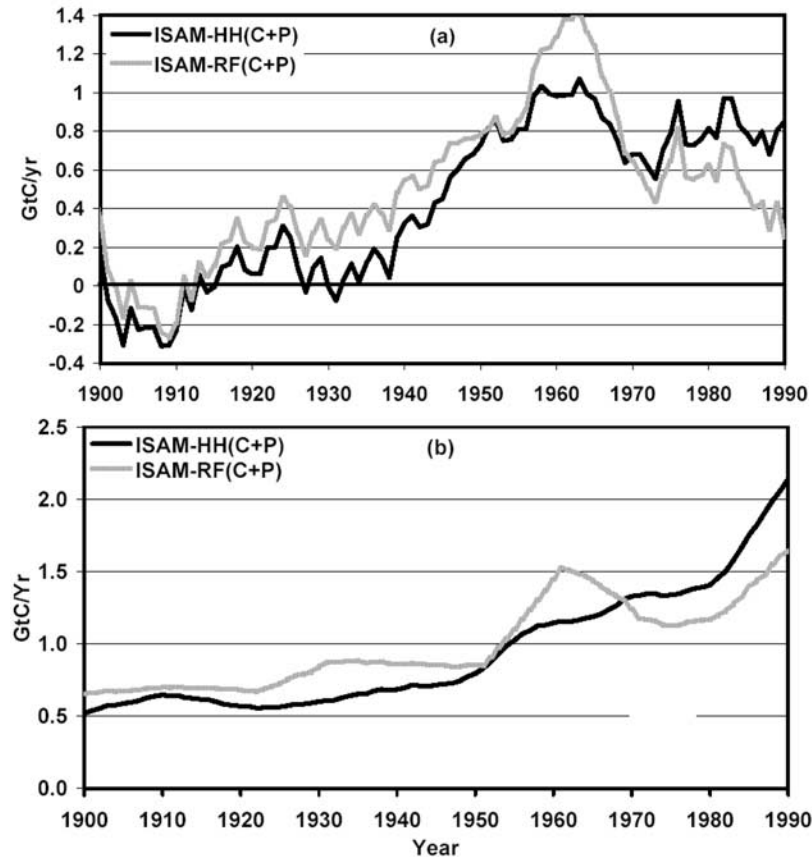
Figure 14. ISAM estimated (a) net land-atmosphere flux, and (b) land use sources between 1900 and 2000 associated with climate, CO_2 increase, and cropland and pastureland changes. For the ISAM-HH (C + P) case the croplands and pasturelands changes data are taken from *Houghton and Hackler* [1999, 2001] and *Houghton* [1999, 2000, 2003], whereas for the ISAM-RF(C + P) case the cropland data are based on *Ramankutty and Foley* [1998, 1999], and pastureland data are based on *Houghton and Hackler* [1999, 2001] and *Houghton* [1999, 2000, 2003].

sink were 0.43 GtC to 0.83 GtC/yr (0.63 GtC/yr was middle of the range value).

[66] Although our model estimated range of values for land use emissions, and the lower range of values for the net land-atmosphere flux, fall within the range of those estimated by IPCC (2001) (land use emissions: 0.6 to 2.5 GtC/yr; net land-atmosphere flux: −0.9 to 0.5GtC/yr), our model estimated upper range of value for net land atmosphere flux is outside the range of the IPCC estimated values. It should be noted that our land use analysis does not consider wood harvest, and shifting cultivation activities. According to *Houghton* [2003], wood harvest and shifting cultivation activities were responsible for about 20% of the total land use emissions in 1980s. Incorporating these additional land use activities in the ISAM would likely to lead much higher ISAM estimated land use emissions and even much less carbon sink strength for the 1980s.

5. Concluding Remarks

[67] Over the period 1900–1950, our terrestrial ISAM model results for the land use flux based on two different sets of land use data for cropland changes (HH and RF) exhibited similar trends (Figure 5d). However, the results were substantially different thereafter, particularly after around 1960 when the fluxes based on HH data show a constant increasing trend until 1990, whereas the fluxes based on RF data show a sharp decreasing trend. The increasing net land uptake of atmospheric CO_2 based on the RF data set during the 1980s is mainly due to this decline in the net land use source during the 1980s (Figure 5d), which does not occur in the HH data due to higher deforestation rates. If the land use emissions are indeed higher, such as in the case of HH data, the terrestrial ecosystems may not act as a sink for atmospheric CO_2 as suggested by the most recent IPCC assessment [*Prentice et al.*, 2001] and some other recent studies [*Bousquet et al.*, 2000; *House et al.*, 2003]. However, if the terrestrial biosphere was indeed acting as a sink for atmospheric CO_2, then the magnitude of our model estimated net terrestrial sink may be underestimated or land use emissions are overestimated.

[68] A number of processes that may enhance the ISAM net terrestrial sink processes and might lower the land-atmosphere flux values include: the contribution of nitrogen deposition [*Prentice et al.*, 2001, and references therein];

fire suppression leading to woody encroachment [*Houghton et al.*, 1999]; recovery from past natural disturbances, sedimentation, and spatial redistribution of carbon in products [*House et al.*, 2003]; and uptake of carbon during weathering processes on land and transport of carbon from land areas to the ocean via rivers [*Prentice et al.*, 2001]. Consideration of these processes is beyond the scope of the present analysis but may be significant for additional carbon sink and should be considered in development of more detailed models.

[69] In regard to the land cover change data used in this study, we believe that large uncertainty in these two sets of data, which provides extreme high and low estimates of land clearing for croplands, merits comprehensive investigation. The causes for differences will require analysis using the full range of environmental monitoring at all scales, including integration of the recent land cover changes in forest cover with high resolution satellite measurements. Some of these efforts are already underway. For example, two recent studies of tropical deforestation based on satellite data [*Achard et al.*, 2002; *DeFries et al.*, 2002] suggest that the FAO-based rates of deforestation in tropical forests might be overestimated. *Achard et al.* [2002] found rates 23% lower than the FAO for the 1990s, while *DeFries et al.* [2002] estimated 54% lower than those reported by the FAO. However, in his most recent paper, *Houghton* [2003] questioned the inconsistency between these two studies. *Houghton* [2003] pointed out that the estimates of rates of change based on these two studies are as different from each other as they are from those of the FAO. He also questioned the reliability of the satellite based percent tree cover data of *DeFries et al.* [2002] for tropical Africa, where the greatest differences are found [*Houghton*, 2003]. *DeFries et al.* [2002] have also noted that tropical Africa is the most uncertain region because of difficulties in detecting patchy clearings and spurious data sources. There is an urgent need for a network of ground and satellite-based long-term monitoring plans to measure changes in the forest cover at the local level. Such programs will be necessary to make reliable global emissions estimates from changes in forest covers.

[70] In conclusion, our results leave open the possibility that the discrepancy in the magnitudes of the modeled and the data-based net land atmosphere fluxes may be due to the limitations of terrestrial ecosystem models or the overestimation of the land use sources. Finding the missing sink in the terrestrial biosphere will require continued refinements of both terrestrial biospheric sink capacity and/or the global land use emission estimates from changes in forest covers, or refinement of O_2 and CO_2 based estimates.

References

Achard, F., H. D. Eva, H. J. Stibig, P. Mayaux, J. Gallego, T. Richards, and J. P. Malingreau (2002), Determination of deforestation rates of the world's humid tropical forests, *Science*, 297, 999–1002.

Bacastow, R. B., and C. D. Keeling (1973), Atmospheric carbon dioxide and radiocarbon in the natural carbon cycle: II. Changes from A.D. 1700 to 2070 as deduced from a geochemical model, in *Carbon and the Biosphere*, edited by G. Woodwell and E. Pecan, pp. 86–134, U.S. Atomic Energy Comm., Washington, D. C.

Batjes, N. H. (1996), Total carbon and nitrogen in the soils of the world, *Eur. J. Soil Sci.*, 47, 151–163.

Bolin, B., R. Sukumar, P. Ciais, W. Cramer, P. Jarvis, H. Kheshgi, C. Nobre, S. Semenov, and W. Steffen (2000), Global perspective, in *Land Use, Land-Use Change, and Forestry: A Special Report of the IPCC*, edited by R. T. Watson et al., pp. 23–51, Cambridge Univ. Press, New York.

Bousquet, P., P. Peylin, P. Ciais, C. Le Quéré, P. Friedlingstein, and P. P. Tans (2000), Regional changes of CO_2 fluxes over land and oceans since 1980, *Science*, 290, 1342–1346.

Cramer, W., et al. (1999), Comparing global models of terrestrial net primary productivity (NPP): Overview and key results, *Global Change Biol.*, 5, 1–15.

Cramer, W., et al. (2001), Global response of terrestrial ecosystem structure and function to CO_2 and climate change: Results from six dynamic global vegetation models, *Global Change Biol.*, 7, 357–373.

Davidson, E. A., and I. L. Ackerman (1993), Changes in soil carbon inventories following cultivation of previously untilled soils, *Biogeochemistry*, 20, 161–193.

DeFries, R. S., R. A. Houghton, M. C. Hansen, C. B. Field, D. Skole, and J. Townshend (2002), Carbon emissions from tropical deforestation and regrowth based on satellite observations for the 1980s and 1990s, *Proc. Natl. Acad. Sci. U. S. A.*, 99(22), 14,256–14,261.

Enting, I. G., T. M. L. Wigley, and M. Heimann (Eds.) (1994), Future emissions and concentrations of carbon dioxide: Key ocean/atmosphere/land analyses, *Tech. Pap. 31*, CSIRO Div. of Atmos. Res., Melbourne, Victoria, Australia.

Eswaren, H., E. van der Berg, and P. Reich (1993), Organic carbon in soils of the world, *Soil Sci. Soc. Am. J.*, 57, 192–194.

Farquhar, G. D., and S. von Caemmerer (1982), Modelling of photosynthetic response to environmental conditions, in *Encyclopedia of Plant Physiology: New Series*, vol. 12B, *Physiological Plant Ecology II: Water Relations and Carbon Assimilation*, edited by O. L. Lange et al., pp. 549–588, Springer, New York.

Friedli, H., H. Lötscher, H. Oeschger, U. Siegenthaler, and B. Stauffer (1986), Ice core record of $^{13}C/^{12}C$ ratio of atmospheric CO_2 in the past two centuries, *Nature*, 324, 237–238.

Gates, D. M. (1985), Global biospheric response to increasing atmospheric carbon dioxide concentration, in *Direct Effects of Increasing Carbon Dioxide on Vegetation*, edited by B. R. Strain and J. D. Cure, *DOE/ER-0238*, pp. 171–184, Carbon Dioxide Res. Div., U.S. Dep. of Energy, Washington, D. C.

Gitz, V., and P. Ciais (2003), Amplifying effects of land-use change on atmospheric CO_2 levels, *Global Biogeochem. Cycles*, 17(1), 1024, doi:10.1029/2002GB001963.

Haxeltine, A., and I. C. Prentice (1996), BIOME3: An equilibrium terrestrial biosphere model based on ecophysiological constraints, resource availability, and competition among plant functional types, *Global Biogeochem. Cycles*, 10, 693–709.

Houghton, R. A. (1999), The annual net flux of carbon to the atmosphere from changes in land use 1850–1990, *Tellus, Ser. B*, 51, 298–313.

Houghton, R. A. (2000), A new estimate of global sources and sinks of carbon from land-use change, *Eos Trans. AGU*, 81(19), Suppl. S281.

Houghton, R. A. (2003), Revised estimates of the annual net flux of carbon to the atmosphere from changes in land use 1850–2000, *Tellus, Ser. B*, 55, 378–390.

Houghton, R. A., and J. L. Hackler (1999), Emissions of carbon from forestry and land-use change in tropical Asia, *Global Change Biol.*, 5, 481–492.

Houghton, R. A., and J. L. Hackler (2001), Carbon flux to the atmosphere from land-use changes: 1850 to 1990, *ORNL/CDIAC-131*, 86 pp., Carbon Dioxide Inf. Anal. Cent., Oak Ridge Natl. Lab., Oak Ridge, Tenn. (Available at http://cdiac.esd.ornl.gov/ndps/ndp050.html)

Houghton, R. A., J. E. Hobbie, J. M. Melillo, B. Moore, B. J. Peterson, G. R. Shaver, and G. M. Woodwell (1983), Changes in the carbon content of terrestrial biota and soils between 1860 and 1980—A net release of CO_2 to the atmosphere, *Ecol. Monogr.*, 53, 235–262.

Houghton, R. A., J. L. Hackler, and K. T. Lawrence (1999), The US carbon budget: Contributions from land-use change, *Science*, 285, 574–578.

House, J. I., I. C. Prentice, N. Ramankutty, R. A. Houghton, and M. Heimann (2003), Reconciling apparent inconsistencies in estimates of terrestrial CO_2 sources and sinks, *Tellus, Ser. B*, 55, 345–363.

Jain, A. K., and K. A. S. Hayhoe (2003), Global air pollution problems, in *Handbook of Atmospheric Sciences*, edited by C. N. Hewitt and A. V. Jackson, pp. 339–371, Blackwell Sci., Malden, Mass.

Jain, A. K., H. S. Kheshgi, M. I. Hoffert, and D. J. Wuebbles (1995), Distribution of radiocarbon as a test of global carbon-cycle models, *Global Biogeochem. Cycles*, *9*, 153–166.

Jain, A. K., H. S. Kheshgi, and D. J. Wuebbles (1996), A globally aggregated reconstruction of cycles of carbon and its isotopes, *Tellus, Ser. B*, *48*, 583–600.

Jain, A. K., H. S. Kheshgi, and D. J. Wuebbles (1997), Is there an imbalance in the global budget of bomb-produced radiocarbon?, *J. Geophys. Res.*, *102*, 1327–1333.

Jenkinson, D. S. (1990), The turnover of organic carbon and nitrogen in soil, *Philos. Trans. R. Soc. London, Ser. B*, *329*, 361–368.

Jobbagy, E., and R. B. Jackson (2000), The vertical distribution of soil organic carbon and its relation to climate and vegetation, *Ecol. Appl.*, *10*(2), 423–436.

Keeling, C. D., and T. P. Whorf (2000), Atmospheric CO_2 records from sites in the SIO air sampling network, in *Trends: A Compendium of Data on Global Change*, pp. 1–28, Carbon Dioxide Inf. Anal. Cent., Oak Ridge Natl. Lab., Oak Ridge, Tenn.

Keeling, C. D., R. B. Bacastow, and T. P. Whorf (1982), Measurements of the concentration of carbon dioxide at Mauna Loa Observatory, Hawaii, in *Carbon Dioxide Review: 1982*, edited by W. C. Clark, pp. 377–385, Oxford Univ. Press, New York.

Kheshgi, H. S., and A. K. Jain (2003), Projecting future climate change: Implications of carbon cycle model intercomparison, *Global Biogeochem. Cycles*, *17*(2), 1047, doi:10.1029/2001GB001842.

Kheshgi, H. S., A. K. Jain, and D. J. Wuebbles (1996), Accounting for the missing carbon sink with the CO_2 fertilization effect, *Clim. Change*, *33*, 31–62.

Kheshgi, H. S., A. K. Jain, and D. J. Wuebbles (1999), The global carbon budget and its uncertainty derived from carbon dioxide and carbon isotopes, *J. Geophys. Res.*, *104*, 31,127–31,144.

King, A. W., W. R. Emanuel, S. D. Wullschleger, and W. M. Post (1995), In search of the missing carbon sink: A model of terrestrial biospheric response to land-use change and atmospheric CO_2, *Tellus, Ser. B*, *47*, 501–519.

Klein Goldewijk, C. G. M. (2001), Estimating global land use change over the past 300 years: The HYDE 2.0 database, *Global Biogeochem. Cycles*, *15*, 417–433.

Loveland, T. R., and A. S. Belward (1997), The IGBP-DIS global 1 km land cover data set, DISCover: First results, *Int. J. Remote Sens.*, *18*, 3291–3295.

Marland, G., et al. (2003), The climatic impacts of land surface change and carbon management, and the implications for climate-change mitigation policy, *Clim. Policy*, *3*, 149–157.

McGuire, A. D., et al. (2001), Carbon balance of the terrestrial biosphere in the twentieth century: Analyses of CO_2, climate and land-use effects with four process-based ecosystem models, *Global Biogeochem. Cycles*, *15*(1), 183–206.

Melillo, J. M., A. D. McGuire, D. W. Kicklighter, B. Moore III, C. J. Vorosmarty, and A. L. Schloss (1993), Global climate change and terrestrial net primary production, *Nature*, *363*, 234–239.

Neftel, A., E. Moor, H. Oeschger, and B. Stauffer (1985), Evidence from polar ice cores for the increase in atmospheric CO_2 in the past two centuries, *Nature*, *315*, 45–47.

Pacala, S. W. (2001), Consistent land- and atmosphere-based US carbon sink estimates, *Science*, *292*, 2316–2320.

Pastor, J., and W. M. Post (1985), Development of a linked forest productivity-soil process model, *Tech. Rep. ORNL/TM-9519*, Oak Ridge Natl. Lab., Oak Ridge, Tenn.

Polglase, P. J., and Y. P. Wang (1992), Potential CO_2-enhanced carbon storage by the terrestrial biosphere, *Aust. J. Bot.*, *40*, 641–656.

Post, W. M., W. R. Emanuel, P. J. Zinke, and A. G. Stangenberger (1982), Soil carbon pools and world life zones, *Nature*, *298*, 156–159.

Post, W. M., A. W. King, and S. D. Wullschleger (1997), Historical variations in terrestrial biospheric carbon storage, *Global Biogeochem. Cycles*, *11*, 99–110.

Prentice, C., G. Farquhar, M. Fasham, M. Goulden, M. Heimann, V. Jaramillo, H. Kheshgi, C. L. Quéré, R. Scholes, and D. Wallace (2001), The carbon cycle and atmospheric CO_2, in *Climate Change 2001: The Scientific Basis: Contribution of WGI to the Third Assessment Report of the IPCC*, edited by J. T. Houghton et al., pp. 183–237, Cambridge Univ. Press, New York.

Ramankutty, N., and J. Foley (1998), Characterizing patterns of global land use: An analysis of global croplands data, *Global Biogeochem. Cycles*, *12*, 667–685.

Ramankutty, N., and J. A. Foley (1999), Estimating historical changes in global land cover: Croplands from 1700 to 1992, *Global Biogeochem. Cycles*, *13*, 997–1027.

Ramankutty, N., J. A. Foley, and N. J. Olejniczak (2002), People on the land: Changes in global population and cropland during the 20th century, *Ambio*, *31*, 251–257.

Rawls, W. J., D. L. Brakensiek, and K. E. Saxton (1982), Estimation of soil water properties, *Trans. ASAE*, *25*, 1316–1328.

Ryan, M. G., R. M. Hubbard, S. Pongracic, R. J. Raison, and R. E. McMurtrie (1996), Autotrophic respiration in Pinus radiate in relation to nutrient status, *Tree Physiol.*, *16*, 333–343.

Ryan, M. G., M. B. Lavigne, and S. T. Gower (1997), Annual carbon cost of autotrophic respiration in boreal forest ecosystems in relation to species and climate, *J. Geophys. Res.*, *102*, 28,871–28,883.

Schimel, D., D. Alves, I. Enting, M. Heimann, F. Joos, D. Raynaud, and T. Wigley (1996), CO_2 and the carbon cycle, in *Climate Change 1995: The Science of Climate Change: Contribution of WGI to the Second Assessment Report of the IPCC*, edited by J. T. Houghton et al., pp. 65–86, Cambridge Univ. Press, New York.

Schimel, D. S., et al. (2001), Recent patterns and mechanisms of carbon exchange by terrestrial ecosystems, *Nature*, *414*, 169–172.

Schlesinger, W. H. (1997), *Biogeochemistry: An Analysis of Global Change*, 543 pp., Elsevier, New York.

Thornthwaite, C. W., and J. R. Mather (1957), Instructions and tables for computing potential evapotranspiration and the water balance, *Publ. Climatol.*, *10*, 183–311.

United Nations Framework Convention on Climate Change (1997), Kyoto Protocol to the United Nations Framework Convention on Climate Change, *FCCC/CP/1997/L.7/Add. 1*, Bonn, Germany.

Webb, R. S., C. E. Rosenzweig, and E. R. Levine (1991), A global data set of soil particle size properties, *NASA Tech. Memo.*, *4286*, 34 pp.

Zhu, Z., and E. Waller (2003), Global forest cover mapping for the United Nations Food and Agriculture Organization Forest Resources Assessment 2000 Program, *For. Sci.*, *49*, 369–380.

Zobler, L. (1986), A world soil file for global climate modelling, *NASA Tech. Memo.*, *87802*, 32 pp.

Zobler, L. (1999), Global Soil Types, 1-Degree Grid (Zobler), data set, Distrib. Active Arch. Cent., Oak Ridge Natl. Lab., Oak Ridge, Tenn. (Available at http://www.daac.ornl.gov)

————————————

A. K. Jain and X. Yang, Department of Atmospheric Science, University of Illinois, 105 South Gregory Street, Urbana, IL 61801, USA. (jain@atmos.uiuc.edu)